Evaluación de Riesgos Naturales
- América Latina -
Consultores en Riesgos y Desastres

ERN

CAPRA

CENTRAL AMERICA PROBABILISTIC RISK ASSESSMENT
EVALUACIÓN PROBABILISTA DE RIESGOS EN CENTRO AMÉRICA

BELIZE

TASK I
HAZARD IDENTIFICATION, HISTORICAL REVIEW AND PROBABILISTIC ANALYSIS

TECHNICAL REPORT TASK 1.2
HAZARD MODELS REVIEW AND SELECTION

Evaluación de Riesgos Naturales
- América Latina -
Consultores en Riesgos y Desastres

Colombia
Carrera 19A # 84-14 Of 504
Edificio Torrenova
Tel. 57-1-691-6113
Fax 57-1-691-6102
Bogotá, D.C.

INGENIAR

iTEC
INGENIERIA TECNICA Y CIENTIFICA LTDA

España
Centro Internacional de Métodos Numéricos
en Ingeniería - CIMNE
Campus Nord UPC
Tel. 34-93-401-64-96
Fax 34-93-401-10-48
Barcelona

C I M N E

México
Vito Alessio Robles No. 179
Col. Hacienda de Guadalupe Chimalistac
C.P.01050 Delegación Álvaro Obregón
Tel. 55-5-616-8161
Fax 55-5-616-8162
México, D.F.

ERN Ingenieros Consultores, S. C.

ERN Evaluación de Riesgos Naturales – América Latina
www.ern-la.com

Direction and Coordination of Technical Working Groups – Consortium ERN America Latina

Omar Darío Cardona A.
Project General Direction

Luis Eduardo Yamín L.
Technical Direction ERN (COL)

Mario Gustavo Ordaz S.
Technical Direction ERN (MEX)

Alex Horia Barbat B.
Technical Direction CIMNE (ESP)

Gabriel Andrés Bernal G.
General Coordination ERN (COL)

Eduardo Reinoso A.
General Coordination ERN (MEX)

Martha Liliana Carreño T.
General Coordination I CIMNE (ESP)

Specialists and Advisors – Working Groups

Julián Tristancho
Specialist ERN (COL)

Carlos Eduardo Avelar F.
Specialist ERN (MEX)

Mabel Cristina Marulanda F.
Specialist CIMNE(SPN)

Miguel Genaro Mora C.
Specialist ERN (COL)

Benjamín Huerta G.
Specialist ERN (MEX)

Jairo Andrés Valcárcel T.
Specialist CIMNE(SPN)

César Augusto Velásquez V.
Specialist ERN (COL)

Mauro Pompeyo Niño L.
Specialist ERN (MEX)

Juan Pablo Londoño L.
Specialist CIMNE(SPN)

Karina Santamaría D.
Specialist ERN (COL)

Isaías Martínez A.
Technical Assistant ERN (MEX)

René Salgueiro
Specialist CIMNE(SPN)

Mauricio Cardona O.
Specialist ERN (COL)

Edgar Osuna H.
Technical Assistant ERN (MEX)

Nieves Lantada
Specialist CIMNE(SPN)

Sergio Enrique Forero A.
Specialist ERN (COL)

José Juan Hernández G.
Technical Assistant ERN (MEX)

Álvaro Martín Moreno R.
Associated Advisor (COL)

Mario Andrés Salgado G.
Technical Assistant ERN (COL)

Marco Torres
Associated Advisor (MEX)

Mario Díaz-Granados O.
Associated Advisor (COL)

Juan Pablo Forero A.
Technical Assistant ERN (COL)

Johoner Venicio Correa C.
Technical Assistant ERN (COL)

Liliana Narvaez M.
Associated Advisor (COL)

Andrés Mauricio Torres C.
Technical Assistant ERN (COL)

Juan Miguel Galindo P.
Technical Assistant ERN (COL)

Juan Camilo Olaya
Technical Assistant ERN (COL)

Diana Marcela González C.
Technical Assistant ERN (COL)

Yinsury Sodel Peña V.
Technical Assistant ERN (COL)

Steven White
Technical Assistant ERN (COL)

Local Advisors

SNET **Francisco Ernesto Durán & Giovanni Molina El** Salvador

Osmar E. Velasco
Guatemala

Oscar Elvir Honduras
Romaldo Isaac Lewis Belize

Interamerican Development Bank

Flavio Bazán
Sectorial Specialist

Cassandra T. Rogers
Sectorial Specialist

Sergio Lacambra
Sectorial Specialist

Tsuneki Hori
Internal Consultant

Oscar Anil Ishizawa
Internal Consultant

World Bank

Francis Ghesquiere
Coordinador Regional

Joaquín Toro
Specialist

Fernando Ramírez C.
Specialist

Edward C. Anderson
Specialist

Stuart Gill
Specialist

Table of Contents

Ilustrations index

Table index

1 Evaluation model for seismic hazard

1.1 Introduction

The danger arising from seismic activity in places close to human settlements or population centres has led to a need to establish parameters to define the level of hazard, and general methods which will allow those parameters to be estimated.

The parameters that define the level of danger in a seismic hazard model are known as *strong movement* parameters. These parameters define the intensity of movement at the place of analysis. The estimate is made through equations known as *attenuation functions*, which depend principally on the distance from the seismogenic source to the site, the magnitude of the earthquake, and the type of focal mechanism of rupture.

1.2 Estimate of parameters of strong motion

One of the principal components of an analysis of seismic hazard is the study of the attenuation function of parameters of intensity which characterise movement.

1.2.1 *Effects of magnitude and distance*

Much of the energy of an earthquake is released in the form of waves of mechanical effort which move through the earth's cortex. Given that magnitude is related to the energy released at the focus of the earthquake, the intensity of these waves is related to magnitude. The principal effect of magnitude is an increase in the amplitude of intensity, a variation in frequency content, and an increase in the direction of vibration.

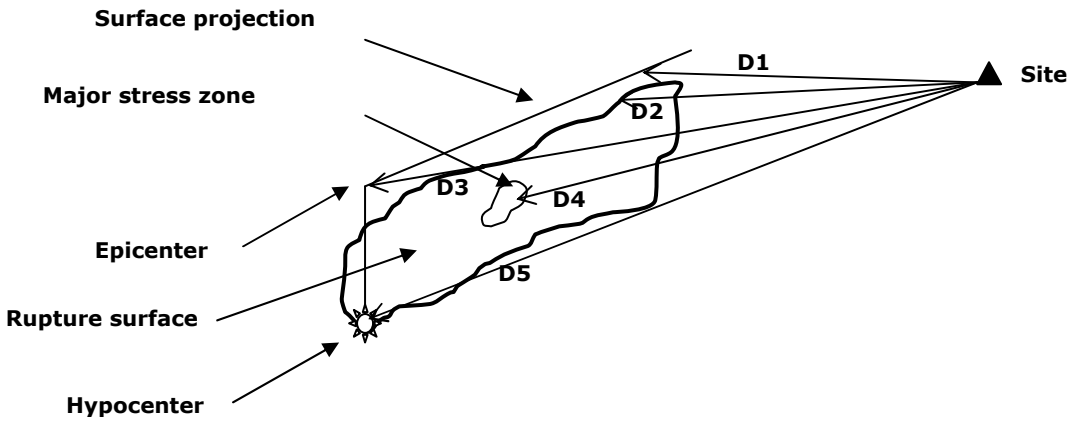

Figure 1-1
Example of several measurements of distances used in attenuation functions.
(Source: Taken from Kramer S., Geotechnical Earthquake Engineering., Ed. Prentice Hall., 1996)

1.2.2 *Estimate of parameters of amplitude*

The estimate of parameters of amplitude is made on the basis of regressions, starting with sets of historical data in areas with good seismic instrumentation. The following are some important models for prediction.

1.2.2.1 *Maximum acceleration*

Maximum acceleration is the parameter most commonly used in seismic hazard studies, to represent the movement of the ground, and a number of models have been proposed for the attenuation of this parameter over distance and the properties of the means of transmission. The greater the quantity of seismic records, the more refined the attenuation functions will be, and this has meant that there had been several publications of new and more refined correlations. The level of refinement increases as methods are developed for more advanced processing.

1.2.2.2 *Ordinates in the response spectrum*

Climent et al, 1994 and Schmidt et al, 1987 developed spectral functions for attenuation of pseudo-velocity for 0.25, 0.5, 1.0, 2.0, 5.0, 10.0 and 40 Hz. The coefficients associated with the attenuation of these spectral ordinates may be consulted in those studies.

1.3 General methods to calculate the hazard

The definition of seismic hazard uses the definitions and methods presented above, to establish the level of danger expected in a given site or area. Under the influence of seismic activity from identified sources nearby. Historically, engineers, geologists and seismologists have been concerned to develop methods of calculation which will increasingly improve representation of the comportment of sources increasingly better, and the passage of waves through a rocky medium, the response of soils and the structural response at the site of interest. Hence, it is possible to identify two main methods for the evaluation of the hazard, which bring together efforts made in the past in different studies around the world.

1.3.1 *Deterministic analysis of seismic hazard*

For many years, the deterministic seismic hazard analysis (DSHA) was the prime tool in seismic engineering for assessing the hazard in a given zone. The use of DSHA implies the definition of a particular scenario on which the estimated movement of the ground is based, with the related secondary effects. The scenario is defined as an earthquake of a known magnitude, which takes place at a certain site. Steps to arrive to apply DHSA are:

1. The characterization of sources generating earthquakes with an influence at the site taken for analysis. Each source has to be defined in terms of its geometry and seismicity

2. Selection of the distance from the source to the site. Generally, the shortest distance between the source and the site of analysis is taken.

3. Selection of the earthquake to analyse, which represents as nearly as possible the seismic potential of the source considered, in terms of intensity at the site under study. This is chosen based on a comparison of intensity levels generated by historical earthquakes in the region, or in other regions with similar neo-tectonic characteristics, so that it may be possible to define the magnitude of the earthquake analysed for the distances defined in advance.

4. Selection of the attenuation functions which will allow the hazard to be completely characterised at the site. Depending on the scope of the analysis, the attenuation functions will be required for acceleration, velocity, displacement, spectral components of these parameters, duration, and other.

1.3.2 *Probabilistic analysis of seismic hazard*

In recent decades, a probabilistic approach has been developed in the analysis of seismic hazard, in order to include in the analysis the uncertainty associated with variables which are inherent to the seismic danger in a defined region. Parameters such as the frequency of occurrence of a given earthquake, the probability that it will occur at a specific place, probabilities of excedence of seismic intensities, etc, are included in the calculation models, to form a probabilistic seismic hazard analysis (PSHA). The steps to be followed to apply PSHA are:

1. The characterisation of the sources generating earthquakes with an influence on the site analysed, in terms of geometry and distribution of probability of starting points for the rupture in the area of the fault defined. It is usual to assume a uniform probability distribution, which implies that the occurrence of an earthquake can be expected with the same probability in any place in the geometry of the defined source.

2. Determination of seismicity in sources considered, based on historical records of events occurring in the defined geometry (seismic catalogue), and on information and studies of neo-tectonics and palaeoseismology for the source. Seismicity is established through magnitude recurrence curves

3. Selection of attenuation functions which will allow the hazard at the site to be completely characterised. Depending on the scope of the analysis, attenuation functions will be required for acceleration, velocity, displacement, spectral components of these parameters, duration, etc.

4. Finally, the uncertainties associated with location, size and attenuation are combined, and a hazard curve is obtained. This indicates the probability that a specific intensity may be equalled or exceeded in a given period of time.

1.4 Analytical model proposed

1.4.1 *General*

Central America is a zone with a high seismic hazard, principally influenced by the interaction of the Coco and Caribbean plates in the subduction zone of the Pacific. In this study, a method of calculation of the hazard has been developed based on classical seismological theory. Based on the seismicity of sources in the territory, and the laws of attenuation of the various seismic parameters, it is possible to identify seismic hazard for all sources which may have important effects on the region or specific seismic scenarios. The fundamental result of this type of analysis of the rates of excedence is associated with specific recurrence periods.

1.4.2 *Selection*

As a general method of calculation, the probabilistic hazard model is selected, given that it allows scenarios of the occurrence of earthquake to be defined, characterised through the probability of occurrence, and permits appropriate treatment of the uncertainty of the problem. The estimate of the parameters for strong movement is made through the attenuation functions defined in the regional project RESIS II (Norsar et al. 2008), which match the tectonic characteristics of Central America.

1.4.3 *Analysis procedure*

Figure 1-2 presents a flow diagram with the principal elements of the seismic hazard model applied. The main steps of the method used are the following:

(1) *Definition and characterisation of seismogenic:* sources based on geological and neo-tectonic information collected, and earlier studies: a geometrical definition is made of the principal seismogenic sources

(2) *Allocation of parameters and seismicity to different seismic sources:* based on the historical seismic catalogue and earlier studies made, and the parameters of seismicity are allocated to each seismogenic source identified.

(3) *Generation of a set of stochastic events compatible with distribution of location, depth, frequency and magnitude,* based on the foregoing information, a set of possible seismic events is generated through sampling based on a recursive division of the geometry of the sources, and allocation of seismicity parameters to each segment, weighting it in accordance with the contribution of that segment to the total area. For each segment, a series of scenarios is generated with different magnitudes, whose probabilities of occurrence are calculated from specific magnitude recurrence curves for that source.

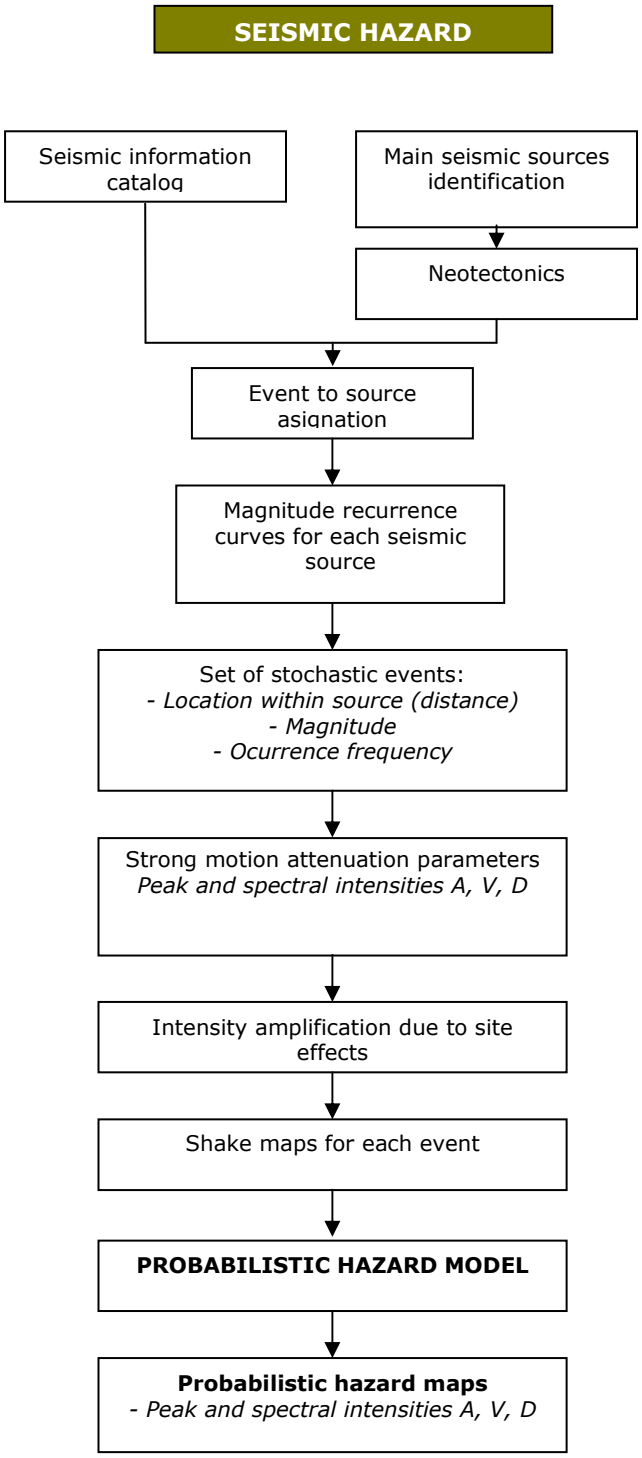

Figure 1-2
Flow diagram of the seismic hazard module.

(4) *Model for attenuation of parameters of ground movement:* the appropriate attenuation functions are defined based on the information collected, previous

studies, and the state of current knowledge of the functions of the spectral attenuation functions.

(5) *Generation of hazard maps for the most important events:* Maps are generated with the spatial distribution of seismic intensity, following maximum spectral values for each stochastic event calculated, through the attenuation model adopted.

(6) *Amplification of hazard parameters due to the effects of the site:* the dynamic response of soil deposits changes the characteristics of amplitude movement, frequency content and duration. The effect of application and de-amplification of the hazard parameters due to the effect of soft surface soil deposits is quantified in a number of ways. Commonly, this is done by shear wave propagation, through soil strata.

(7) *Application of the probabilistic model of seismic hazard:* seismic hazard maps are obtained for different parameters of intensity. The maps are calculated for different return periods in the analysis.

1.4.4 *Seismicity parameters for seismogenic sources*

The activity of the i-th seismic source is specified in terms of the rate of excedence of magnitudes, $\lambda_i(M)$, generated by this source. The magnitude excedence rate measures how often tremors are generated with a magnitude superior to a specific level. For most seismic sources, the function $\lambda_i(M)$, is a modified version of the Gutenberg and Richter ratio. In these cases, seismicity is described as follows:

$$\lambda(M) = \lambda_0 \frac{e^{-\beta M} - e^{-\beta M_u}}{e^{-\beta M_0} - e^{-\beta M_u}} \qquad \textbf{(Ec. 1)}$$

Where M_o is the minimum relevant magnitude, λ_0, β_i, and M_u are parameters that define the rate of excedence of each of the seismic sources. These parameters are different for each source and are estimated by statistical procedures which include information on regions which are tectonically similar to that studied, together with expert information, particularly on the value of M_o, the maximum magnitude which can be generated from each source.

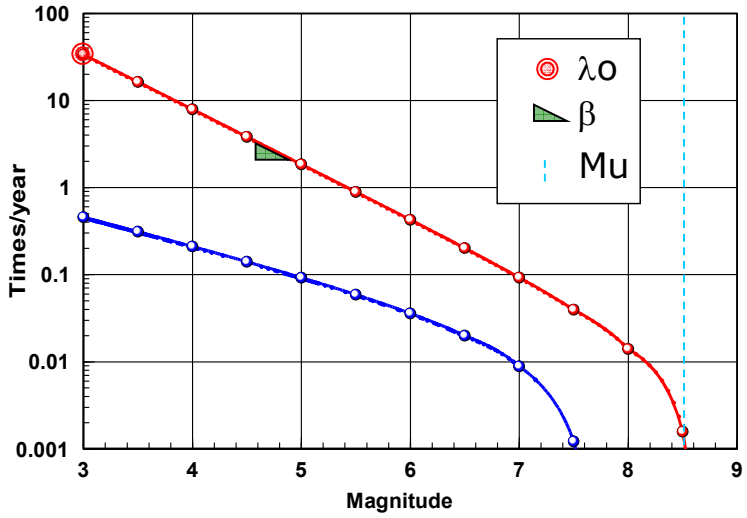

Figure 1-3
Rates of excedence of sources for the Poisson seismicity model

In this way, each of the seismogenic sources is characterised by a series of seismicity parameters, which are determined on the basis of available seismic information. The parameters define the following:

- *Beta value:* identified through the β parameter which represents the slope of the initial segment of the magnitude recurrence curves.

- *Maximum magnitude, M_u:* estimated on the basis of the maximum length of rupture possible from each of the sources, and on the other morphotectonic characteristics.

- *Recurrence rate for earthquakes with a magnitude greater than 4. 0 (λ_0):* this corresponds to the average number of events per year of earthquakes with a magnitude greater than 4.0 produced by a given source

The calculation model for seismic hazard applied on the basis of regional seismogenic sources (intra-plate and subduction faults), in accordance with existing information, and previous studies made in Central America.

1.4.5 *Attenuation of hazard parameters*

Once the rate of activity of each of the seismic sources has been determined, an evaluation must be made of the effects which, in terms of seismic intensity, each of them produces at the site of interest. For this purpose, we need to know what intensity will occur in the case under study, so far supposed to be on the mainland, if a tremor of a given magnitude from the i-th source should occur. The expressions which provide magnitude, source-site relative position and seismic intensity are known as the laws of attenuation. Usually, the relative source-site position is specified by a focal distance, that is, the distance between the seismic focus and site. It is considered that the relevant seismic intensity are the ordinates in the

response spectrum ***a*** (pseudoaccelerations, 5% of critical buffering), quantities which are approximately proportional to the lateral inertial force which is generated on structures during earthquakes.

Special laws of attenuation are used to take account of the fact that attenuation is different for waves of different frequencies, and this makes it possible to calculate the expected response spectrum, given magnitude and distance.

1.4.6 *Calculation of seismic hazard*

Once the seismicity of the sources is known, along with the patterns of attenuation generated in each, the calculation can be made of seismic hazard considering the sum of the effects of all seismic sources and the distance between each source and the site where the structure is located. The hazard expressed in terms of intensity excedence rates ***a***, is calculated with the following expression:

$$\nu(a) = \sum_{n=1}^{N} \int_{Mo}^{Mu} -\frac{\partial \lambda}{\partial M} \Pr(A > a \mid M, R_i) dM \qquad \textbf{(Ec. 2)}$$

Where the sum includes the totality of seismic sources *N*, and $Pr(A>\mathbf{a}|M,R_i)$ there is the probability that intensity will exceed a certain value, given the magnitude of the earthquake M, and the distance between the i-th source and the site R_1. The functions $\lambda_i(M)$ are the rates of activity of seismic sources. The integral is produced from M_o to M_u, which indicates that the contribution of all magnitudes will be taken into account for each seismic source.

Since we suppose that, given the magnitude and the distance, intensity has a lognormal distribution, the probability $Pr(A>a|M, R_i)$ is calculated as follows:

$$\Pr(A > a \mid M, Ro) = \phi\left(\frac{1}{\sigma_{Lna}} \ln \frac{E(A \mid M, R_i)}{a}\right) \qquad \textbf{(Ec. 3)}$$

And φ ( ) is the normal standard distribution, $E(A|M, R_i)$ is the expected value of the logarithm of intensity (given by the related law of attenuation), and y σ_{Lna}. is the related standard deviation.

1.4.7 *Modification of hazard parameters due to the effects of the site*

During an earthquake there are mainly two types of site response which can produce problems in analysis. One is where the soil modifies frequency content and the amplitude of the earthquake, making it more or less destructive. And the other is where the soil itself faults and cracks, moving horizontally and vertically.

The dynamic behaviour of stratified deposits is modelled using spectral transfer functions,

which allow us to know the value of amplification by which spectral acceleration, calculated in terms of firm ground, should be modified. These transfer functions should be constructive for different its maximum acceleration values for firm ground, in order to obtain the non-linear effect of soil degradation. In Figure 1-4 we show a typical spectral transfer function.

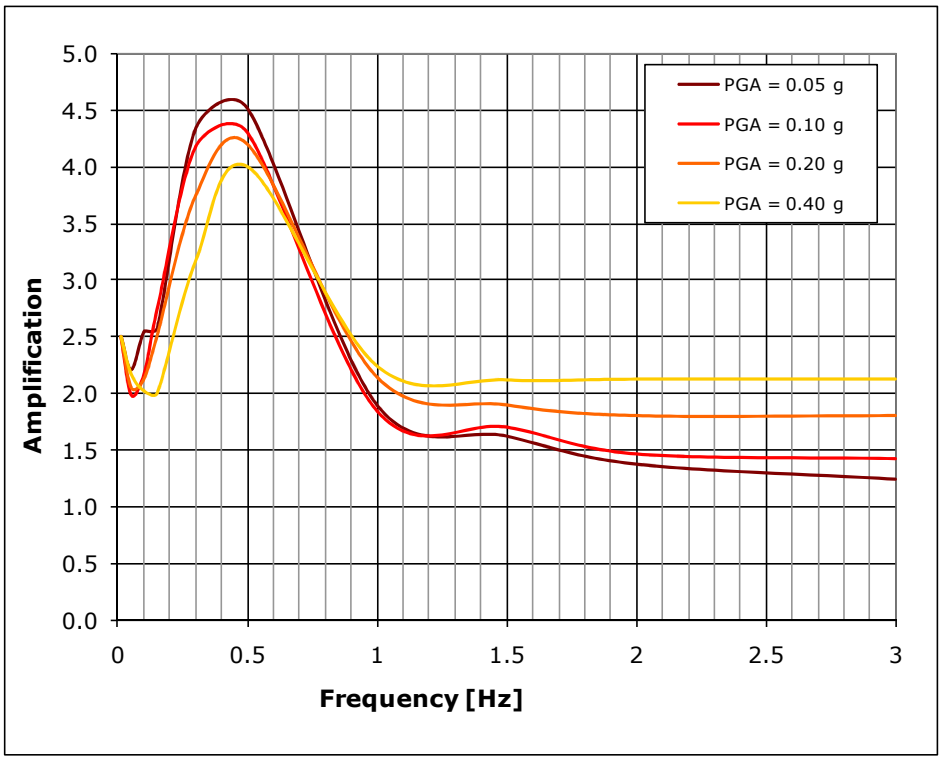

Figure 1-4
Typical spectral amplification function of soft soil

Based on the function of amplification defined by the site analysed, spectral acceleration is at surface level Sa_{sup} calculated as follows:

$$Sa_{sup} = A_{A\max} \cdot Sa_{tf} \qquad \textbf{(Ec. 4)}$$

Where A_{max} is the level of application calculated for a given Amax value (maximum acceleration on firm ground), and Sa_{tf} is the spectral acceleration calculated at ground level, employing the seismic hazard model.

2 Evaluation model for tsunami hazard

2.1 Introduction

The modelling for a tsunami should be approached through two complementary analyses: 1) generation, and 2) propagation and arrival. The analysis of generation allows an estimate to be made of the energy which a detonating event is capable of transmitting to mass of water in the form of gravitational waves. This analysis involves important knowledge of the detonating process, and the capacity to establish or adopt models of behaviour within the expected conditions for the area under study, and the need to establish or adopt models for interaction between the detonating event and the water mass.

2.2 The hidrodynamics of tsunamis

If the conditions in which the tsunami hazard are to be established, we must know the physical characteristics of the displacement of water which earthquakes induce, and which provide the best description of size and destructive capacity. A detailed analytical description can be found in Satake 2002, Helal and Mehanna 2008.

2.2.1 *Long waves*

A system of coordinates is taken, with origin at water in repose at surface level. The geometrical conditions are presented in Figure 2-1, for a wave with a propagation velocity V (vector with components u and w in x and y respectively) (Satake 2002). These waves are also known as gravitational waves, since gravity is what controls the mechanism for restoring the medium.

$$\frac{D\overline{V}}{Dt} = -\overline{g} - \frac{1}{\rho}\nabla p \qquad \textbf{(Ec. 5)}$$

Where

D/Dt indicates the total derived, represented: $\frac{D\overline{V}}{Dt} = \frac{\partial \overline{V}}{\partial t} + \overline{V} \cdot \nabla \overline{V}$

$\nabla \overline{V}$ = Velocity gradients.

$\overline{g}$ = Vector in three components of gravitational acceleration

ρ = Density of the medium of propagation

∇p = Pressure gradient.

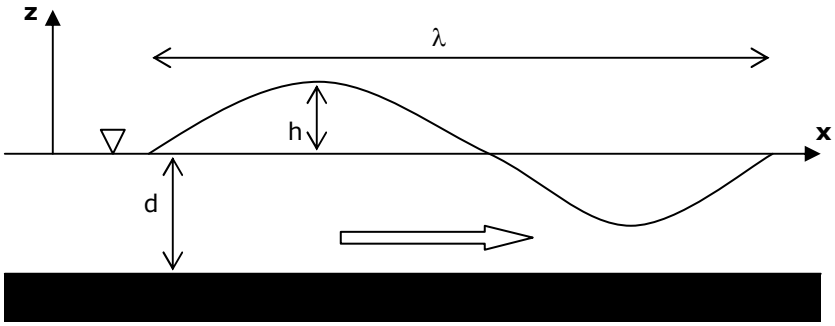

Figure 2-1
Geometrical frame for long waves

In the case of a wavelength λ, where it is much greater than the depth of the medium (λ >>d), the vertical acceleration resulting in the water is negligible in comparison to gravity. This implies that the movement of the water mass in a horizontal direction is almost constant from the bed to the surface. This type of wave is known as *long waves*, or *shallow-water waves*. In the case of tsunamis, ocean depth is typically some 5 km, while the length of the wavefront may be several hundred kilometres. Therefore, the approximation of the long wave is sufficiently valid to characterise the passage of the tsunami´s energy in the open sea.

The component of horizontal movement in Equation 11 can be written as follows, replacing the pressure gradient by the water at surface slope.

$$\frac{Du}{Dt} = -g\frac{\partial h}{\partial x} \qquad \textbf{(Ec. 6)}$$

In the case of a tsunami, the non-linearity term is normally small, and can be discarded ($Du/Dt \approx \partial u/\partial t$), because the movement equation then becomes:

$$\frac{\partial u}{\partial t} = -g\frac{\partial h}{\partial x} \qquad \textbf{(Ec. 7)}$$

In the particular case in which vertical amplitude of movement is small, in comparison to the depth of the water ($d>>h$), the continuity equation can be written as follows:

$$\frac{\partial h}{\partial t} = -\frac{\partial}{\partial x}(du) \qquad \textbf{(Ec. 8)}$$

Waves of this type are known as *low amplitude long linear waves*. The suppositions made are valid to describe the movement of tsunamis, except in regions close to the coast. If we use Equations 13 and 14, we derive the equation for the characteristic wave in this problem, considering that depth d is a constant.

$$\frac{\partial^2 h}{\partial t^2} = c^2 \frac{\partial^2 h}{\partial x^2} \qquad \textbf{(Ec. 9)}$$

where $c = \sqrt{gd}$, corresponding to the velocity of wave propagation

2.2.2 *Wave propagation*

If we suppose that the hydrodynamic behaviour of a tsunami is based on the theory of long waves, we can use the geometrical theory of ray-optical propagation to make an approximate definition of the time taken by the wavefront to arrive at a specific destination. Figure 2-2 presents a wave refraction map for the tsunami that occurred in Indonesia on December 26, 2004[1]

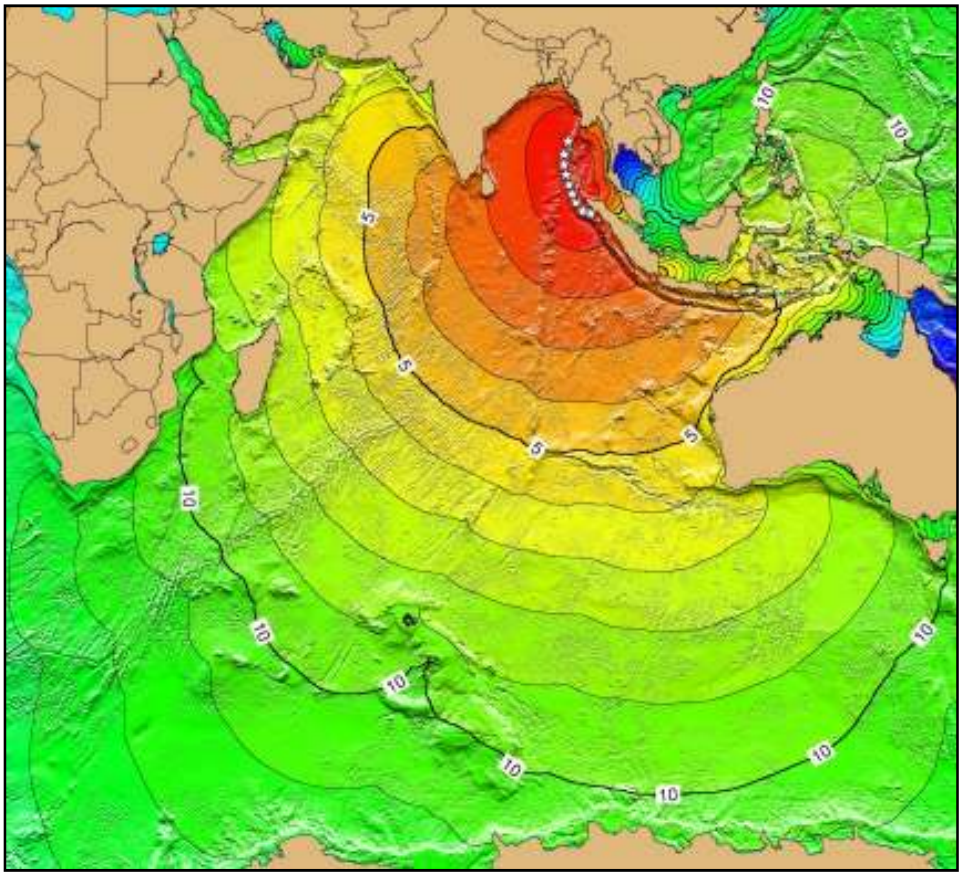

Figure 2-2
Wave refraction diagram with arrival time contours. Indonesian tsunami, December 26, 2004
(Source: National Oceanic and Atmospheric Administration)

[1] Available on the NOAA website

2.2.3 *Green's law*

An analysis of energy conservation along one of the rays of the refraction map allows conditions of approximation to be established for the values proper to the wave generated by the tsunami, obtaining the following expression from the analysis:

$$b_{i-1}\frac{\sqrt{d_{i-1}}}{h_{i-1}^{\ 2}} = b_i\frac{\sqrt{d_i}}{h_i^{\ 2}} \qquad \textbf{(Ec. 10)}$$

Where b is the distance between the rays, d is the depth of the water, and h is the amplitude of the tsunami (amplitude of water, measured from a state of repose). The sub-indices *i-1* and *i*, represent two immediate states of analysis. If we know the amplitude of the tsunami in a certain initial state, together with the characteristics of the ocean and wave propagation, we can estimate the amplitude of the next state with the following expression:

$$h_i = h_{i-1}\left(\frac{b_{i-1}}{b_i}\right)^{1/2}\left(\frac{d_{i-1}}{d_i}\right)^{1/4} \qquad \textbf{(Ec. 11)}$$

This relationship is known as Green´s Law. It is a general relationship of wave propagation in shallow waters, and it can be applied to tsunamis. The ratio b/i-b_{i-1} represents the dispersion of rays as the wave propagates. The lines are distributed perpendicularly or along the contours of the wavefront (see Figure 2-2), with a common origin in the seismic epicentre or generating source.

2.2.4 *Long wave equations*

If the effect of rugosity on the ocean bottom is included, along with the Coriolis effect generated by the rotation of the Earth, the equations for long wave movement for a three-dimensional case can be written as follows (Satake, 2002)

$$\begin{aligned}\frac{\partial U}{\partial t}+U\frac{\partial U}{\partial x}+V\frac{\partial U}{\partial y} &= -fV-g\frac{\partial h}{\partial x}-C_f\frac{U\sqrt{U^2+V^2}}{d+h}\\ \frac{\partial V}{\partial t}+U\frac{\partial V}{\partial x}+V\frac{\partial V}{\partial y} &= -fU-g\frac{\partial h}{\partial y}-C_f\frac{V\sqrt{U^2+V^2}}{d+h}\end{aligned} \qquad \textbf{(Ec. 12)}$$

Together with the continuity equation:

$$\frac{\partial h}{\partial t}+\frac{\partial}{\partial x}\left(U\left(h+d\right)\right)+\frac{\partial}{\partial y}\left(V\left(h+d\right)\right)=0 \qquad \textbf{(Ec. 13)}$$

Where f is the Coriolis parameter, C_f is the a dimensional friction coefficient, U and V are average velocities in the directions x and y respectively. Using these ratios, the behaviour

of the waves generated by a tsunami can be modelled, to the extent that we can predict conditions of propagation and arrival.

2.3 Proposed analytical model

2.3.1 *General*

Seismic activity in the ocean induces the existence of an important hazard caused by tsunami-genic events. The constant displacement of tectonic plates and their interaction in subduction zones means that the tsunami hazard is constantly recurring, with the same frequency or probability as earthquake-triggered events.

2.3.2 *Selection*

The detailed hydrodynamic modelling of the passage of gravitational waves in seas and oceans, requires information at a high level of detail, which is at present not available for the region. An appropriate characterisation of co-seismic displacements on the sea-bed, which determine the magnitude of a tsunami event, requires the use of complex seismological models, this application is restricted given the relatively scanty knowledge available of the phenomenon of rupture in the subduction zones during high-magnitude earthquakes. Similarly, the bathymetric details for all the coast of the country or particular regions of interest, are not available, and a survey of this kind would require major efforts and technological developments.

Therefore, a simplified parametric model is selected, calibrated on the basis of existing information of wave elevation for the Nicaraguan tsunami of 1992, which allows the seismic hazard model, selected as the trigger scenario for the tsunami hazard

2.3.3 *Analysis procedure*

Figure 2-3 gives a flow diagram of the model employed to calculate tsunami hazard. The principal steps to be taken into account when applying this method are:

(1) *Preliminary analysis of seismic hazard*. The seismic hazard models proposed used to evaluate the probability occurrence of detonating events for possible tsunamis on the Pacific coast of Central America. For this, parameters of recurrence were defined from the range of associated sources, principally the subduction of the Pacific, or in the MesoAmerican trench.

(2) *Generation of a set of stochastic methods compatible with the distribution of location, depth, frequency and magnitude of detonating events.* This establishes a set of seismic events which are potential generators of tsunamis, for which the conditions of impact on the coast are calculated. Each of these events has an associated probability of occurrence of a seismic detonating event.

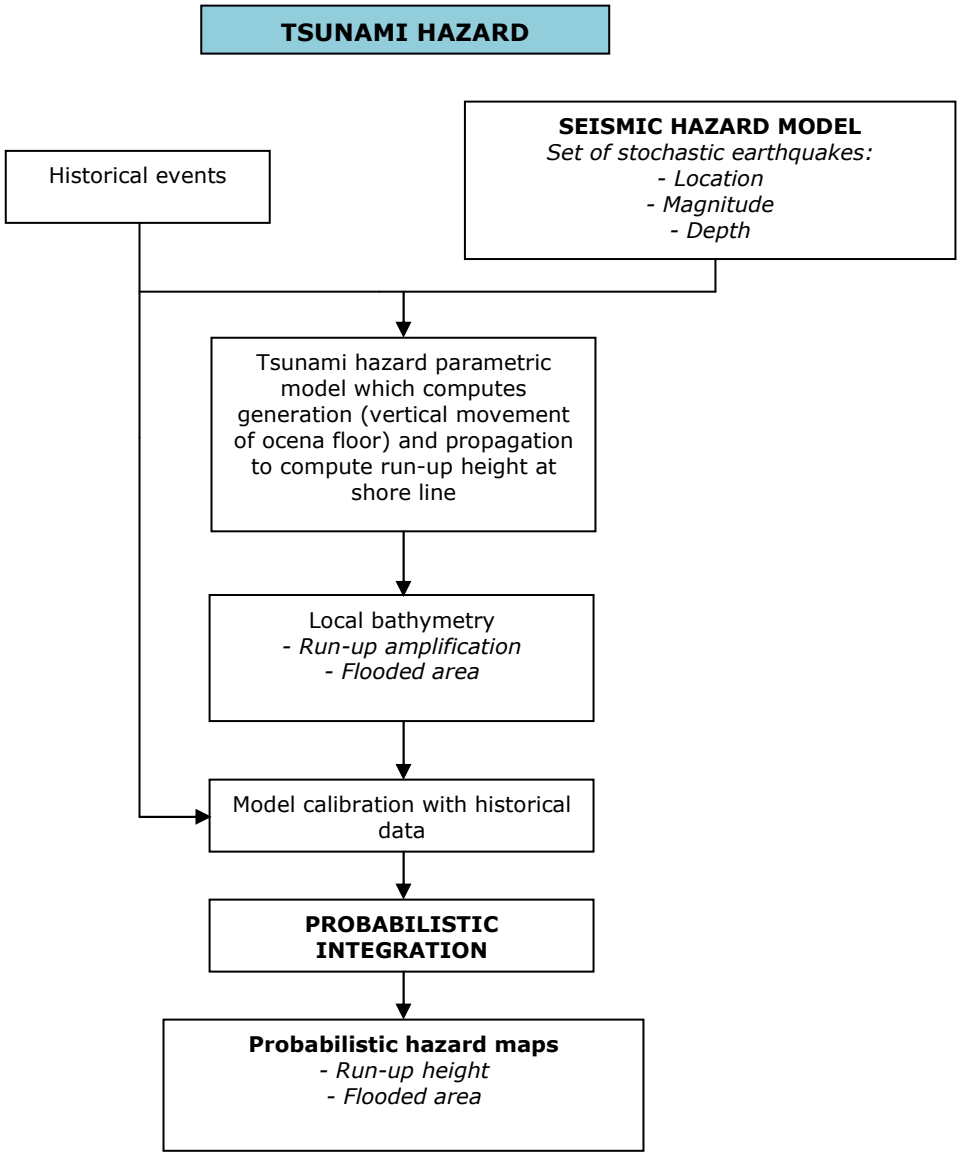

Figure 2-3
Flow diagram of the method proposed

(3) *Parametric model for a tsunami*: Based on the model given below, maximum wave height is determined, and this considers, in simplified form, the principal variables for the generation and propagation of a tsunami.

(4) *Consideration of local bathymetric conditions:* The analysis offers the possibility of including a bathymetric and topographical information base, in as much detail as possible, allowing a determination of specific applications of the effect of a given tsunami.

(5) *Generation of hazard maps for important events*: Spatial distribution maps are generated for wave height, and invasion of the flooding on the mainland, for each stochastic event calculated, through models of generation and propagation adopted. Additionally, calculations can be made of the hazard maps of important historical events.

(6) *Application of the probabiilistic hazard model.* This obtains hazard maps for tsunami, in relation to different parameters of intensity mentioned above, for different return periods.

Throughout the seismic history of Central America, there have been earthquakes with characteristics suited to the generation of tsunamis. Historical cases allow it to be established that, in general, subduction earthquakes of a magnitude greater than 7 are required to trigger a tsunami.

2.3.4 *Description of the parametric model*

Since it would hardly have been practical to model tsunami scenarios using traditional methods of wave generation and propagation, a parametric method was adopted, which simplifies the process the modelling process with reasonable calculation times, but with greater uncertainty in the results. However, due to the probabilistic characteristics of the project, this parametric method was considered acceptable.

The parametric method is based on works of Okal and Synolakis (2004), where, in accordance with observations of maximum height in several important tsunami events, they propose an expression which approximately fits the measurements made along the coast affected. The expression is:

$$\zeta(y) = \frac{b}{\left[\frac{y}{a}\right]^2 + 1} \qquad \textbf{(Ec. 14)}$$

Where $\zeta(y)$ is the wave height, $\boldsymbol{y}$ is the distance from the coast, and a and b are factors obtained in accordance with the characteristics of the tremor. The parameter b is related to the maximum height of the wave, and the parameter a to the distribution of heights on the coast.

Where $\zeta(y)$ is the wave height, $\boldsymbol{y}$ is the distance from the coast, and a and b are factors obtained in accordance with the characteristics of the tremor. The parameter b is related to the maximum height of the wave, and the parameter a to the distribution of heights on the coast.

According to the analysis of several tsunamis produced by earthquakes from a nearby source, Okal and Synolakis (2004) propose values for those parameters. In Figure 2-4 shows a comparison of values obtained with the preceding equation and measurements of maximum height on the Nicaraguan coast produced by the earthquake on September 2,

1992.

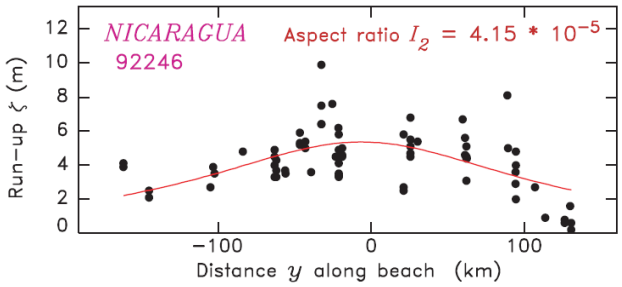

Figure 2-4
Comparison of the model with measurements of the tsunami in Nicaragua, 1992

One additional value related to parameters *a* and *b* is the datum I_2, defined as

$$I_2 = \frac{b}{a} \qquad \textbf{(Ec. 26)}$$

The expressions to obtain the parameters indicated are the result of a process of adjustment of certain events in Mexico and Central America, and the resulting expressions are shown below:

$$b = p_1 Mo^2 + p_2 Mo + p_3 L^2 + p_4 L + p_5 h^2 + p_6 h + p_7 H^2 + p_8 H + p_9 Tan\beta^2 + p_{10} Tan\beta + p_{11}$$
$$I_2 = p_1 Mo^2 + p_2 Mo + p_3 L^2 + p_4 L + p_5 h^2 + p_6 h + p_7 H^2 + p_8 H + p_9 Tan\beta^2 + p_{10} Tan\beta + p_{11} \qquad \textbf{(Ec. 27)}$$

Where Mo is the seismic moment in dyne/centimetres, ***L*** is the minimum distance from the epicentre to the coast in kilometres, ***h*** is the depth of the hypocentre in kilometres, ***H*** is the depth of water in metres, Tanβ is the average slope of the bathymetry starting from the coast, and $\boldsymbol{p_i}$ are adjustment constants for the equations. The values are indicated in Table 2-1.

Table 2-1
Value of p_i-constants for the expressions of "b" and "I_2"

Constants	*b*	I_2
p_1	-9.099E-58	-4.999E-60
p_2	9.919E-29	4.852E-31
p_3	7.250E-06	2.550E-07
p_4	-7.795E-03	-2.047E-04
p_5	-3.071E-04	2.857E-07
p_6	-9.143E-03	-9.571E-05
p_7	-2.500E-08	-7.500E-11
p_8	3.990E-04	1.655E-06
p_9	3.889E+02	3.045E+00
p_{10}	-6.124E+01	-4.430E-01
p_{11}	3.456E+00	5.108E-02

2.3.4.1 *Considerations*

The seismic hazard model proposed is used to generate the variables for the above equations, and this produces a list of events, and magnitude, and the coordinates of the hypocentre. As additional considerations, it is supposed that earthquakes generate tsunamis only if:

a. They have epicentres located in the sea
b. They have magnitude greater than 6
c. The depth of the hypocentre is less than 60 km
d. The maximum distance of affectation is 600 km

Figure 2-5 illustrate some of the variables employed.

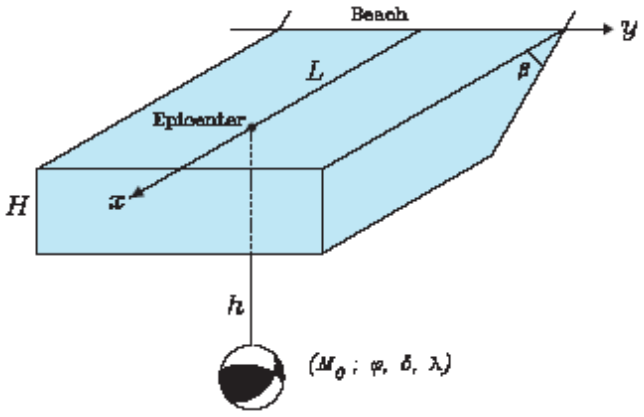

Figure 2-5
Illustrative scheme of variables included in the parametric method.

Additionally, user-defined calculation points are employed. These points indicate the region which interest us to discover the areas flooded by tsunami. They are defined as follows:

1. The coordinates of the coastline (Contour 0)
2. Point on land with approximately in elevation of 15 m (Contour 15). The objective of these points is to make calculations of flood heights, up to their positions.
3. Local amplification factors

It is important for the method that each point on the coast has a corresponding point on land, and that the straight lines obtained with these points do not cross In Figure 2-6 we show a scheme with a definition of these points, and some considerations for the application of the method.

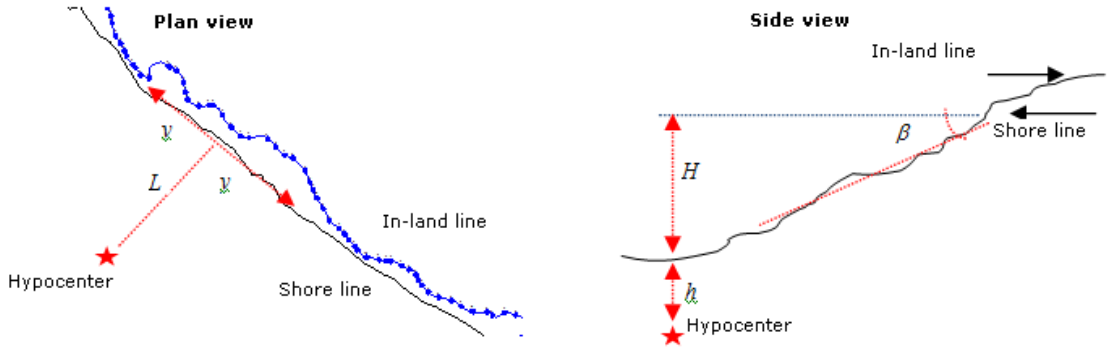

Figure 2-6
Sample considerations for the application of the parametric method

2.3.4.2 *Obtaining parameters*

Given the magnitude of an earthquake, *M*, the seismic moment is obtained with the Hanks and Kalamori 1979 expression of moment.

$$Mo = 10^{(1.5*M+16.1)} \qquad \textbf{(Ec. 28)}$$

With the information of the coordinates of the hypocentre, and the calculation points, the following considerations are applied or for the calculations, illustrated above:

1. Bathymetry information is used to obtain water depth, each, on the epicentre of the earthquake.
2. The closest point to the coast (contour 0) is determined, and the distance between these points is the parameter *L*.
3. Based on this point, the distance "*y*" is obtained for each point.
4. Bathymetry provides the *β* and the tangent value of each point.
5. All of these parameters provide the values of the p_i-constants, to obtain *b* and I_2, and with these values, we obtain the wave height for each point of calculation.

2.3.4.3 *Obtaining flood zones*

Once the wave height ($\zeta(y)$) has been obtained for each calculation, we can obtain the flood zones in each region defined by calculation points, Contours 0 to 15. The estimate of flooded areas is obtained by the difference in wave height seat ($\zeta(y)$), and the elevation of the ground obtained by detailed topography. InFigure 2-7 gives a schematic presentation of this analysis

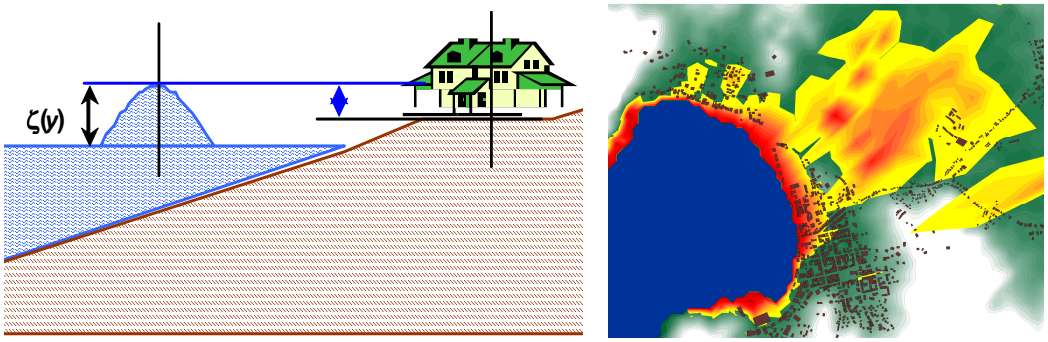

Figure 2-7
Schematic presentation of the estimate of flood heights, and results of flood areas

3 Evaluation model for hurricane hazard

3.1 Introduction

The generation of hurricanes is associated with the incidence of solar radiation on the planet, and climatic processes induced by it. The atmosphere has an average thickness of 130 km and is formed by air of different densities, depending on altitude and position on the Earth's surface. Dry air is composed of 78% nitrogen, 20% oxygen, neon and ozone at less than 1%, with dust and other gases for the remaining 1%. Far more changes can produce water molecules in the composition of the air, which changes its density. The thermal density of the air has an average value of 1.2 kg/m^3, but there may be variations of up to 20%, depending on the time of year and the latitude of the site.

Tropical depressions may or may not develop into relevant events, depending on physical and environmental conditions dominant in the area, and on the moment at which they are generated. When these embryonic tropical depressions find suitable conditions, they can develop and generate tropical storms or hurricanes. All these events are originated in similar meteorological conditions, and exhibit the same life-cycle. The various stages of development of the systems are defined by a *sustained wind velocity*, that is, levels of wind velocity and atmospheric pressure which are maintained for longer than one minute, close to the centre of the system. In the formative stage, the isobaric closed circulation is known as a tropical depression. If the sustained wind velocity exceeds 63 kph (39 mph), this produces a tropical storm. In this stage, the system is already able to produce some type of danger. When winds exceed 119 kph (74 mph), the system is classified as a hurricane, the most severe form of tropical cyclone. The decay of the system occurs when the storm reaches non-tropical waters, or crosses a land mass. If it moves towards a non-tropical environment, it is known as a subtropical storm or subtropical depression. If it moves over a land mass, the winds slow down, and again become storm-class winds (tropical depression), until perhaps they disappear completely.

The potential damage caused by the various processes related to tropical cyclones is directly related to intensity, and always associated with a defined geographical distribution, as follows:

- *Wind:* Hurricane winds may damage or completely destroy vehicles, buildings, roads, etc, and turn refuse and rubble into projectiles which are launched into the air at high speed. For the wind, the parameter used is peak wind velocity for five-second squalls.
- *Tide*: Hurricanes produce an increase in the sea level, which may flood coastal communities. This is the most damaging effect, since 80% of the victims of a cyclone die in the place where the cyclone strikes land. The parameter here is the maximum wave height generated, and the geographical zone of impact.

- *Torrential rain*. Intense rainfall may produce landslides in mountainous areas, and may cause local watercourses to overflow. The intensity-duration-frequency curves are generally used to quantify this.

There are various methods to estimate intensities associated with effects caused by hurricanes. The approach to intensity may be made through *statistical models, dynamic models, or combination of the two.*

3.2 Statistical models

Statistical models are based on the relationship between the characteristics of the storm, and the characteristics of historically observed storms. Given the simplicity, this is much more rapid way of estimating characteristics. At present, the standard model is used as a means of appraising more complex models, such as the dynamic models.

3.3 Dynamic models

The dynamic models based on statistical models are considered to be efficient, although they are less accurate.

Dynamic models are more complex, and require considerably greater computer resources and statistical models, since the matter solved physical equations which govern a natural phenomenon based on a number of numerical methods, and a range of initial conditions determined on the basis of observations of the phenomenon.

US National Weather Service Global Forecast System (GFS)
The system employs the scheme of parameter-setting for the convective effect, known as SAS, a first-order method able to represent conditions of the lowest layer of the atmosphere or PBL, and a hybrid pressure system which varies with altitude. The system is used to forecast the route of a storm.

Limited Area Sine Transform Barotropical (LBAR) model
This is a relatively simple system for predicting the route of a storm. It takes account of only two entry parameters, average wind velocity and altitude, from the GFS system, and frontier conditions.

Global Environmental Multiscale Model (GEM)-Canadian Meteorological Centre (CMC)
This is a global hydrostatic grid, with a resolution of 33 km, to a latitude of 49°. The system requires a high level of computer capability, it employs four variables, and takes account of the initial conditions which are variable over time. The model has a limited capacity to predict the intensity of the system.

European Centre for Medium Range Weather Forecasting (ECMWF),
This is the most complex and most demanding in terms of computer resources, given the resolution, dissemination of data and requirements of the 28 European agencies which form

the system. It was the first system to initialize with four variables. Aside from being a good model to predict the route of a medium-sized tropical storm, the high resolution of the system is useful for predicting intensity.

Navy Operational Global Atmospheric Prediction System (NOGAPS).
This is a global model with a resolution of 55 km and 30 vertical levels, it uses three initializing variables, and like most global models, it is not accurate for estimating the intensity of the system, but is accurate for predicting routes.

NWS Geophysical Fluid Dynamics Model (GFDL) Hurricane model
This is a model limited to a specific region, and has three levels of the resolution., 30 km, 15 km and 7.5 km. This resolution allows the model to resolve smaller characteristics of the system, such as for example the definition and displacement of the eye, or the wall of the storm. It uses 42 vertical levels, and even with available resolution, it cannot fully resolve the complex structure of a hurricane. It is articulated to the Princeton Oceanic Model (POM), which allows oceanic changes to be included, such as ocean surface temperature.

Hurricane Whether Research and Forecasting Model (HWRF)
This was developed by the National Hurricane Prediction Centre, and is a non-hydrostatic model which solves the equation governing the vertical movement of the air, giving the model the ability to represent conditions in the eye of the storm. It uses a horizontal 27 km grid, and 42 vertical levels. Like the GFDL model, it articulates to POM to include variations in ocean conditions.

United Kingdom Meteorological Office (UK NBT) model
This is a non-hydrostatic model, with a resolution in medium latitudes of 40 km, and 50 vertical levels. It is a four-variable entry model, which is applied during three hours prior to starting the process.

3.4 Combined models

As the name suggests, these models are the fruit of a combination of statistical procedures and solutions to the equations which govern the system. Generally, this type of model uses the dynamic of predictions made in numerical models as input, and predicts the behaviour of the storm using statistical relationships based on a compilation of data of historical events. The following are worth mentioning:

NHC91/NHC 98 models
These models - NHC 91 is for the Pacific and NHC 98 for the Atlantic - are combined models because they adopt statistical relationships between the behaviour of a storm, and predictions of dynamic models such as GFS.

Statistical Hurricane Intensity Prediction Scheme (SHIPS)
This model, because it obtains predictions from persistent dynamic and climatological models, provides results on the intensity of the system with errors of less than 10% in

relation to those presented in the model described above SHIFR05.

Decay-SHIPS
This corresponds to the same model as above, with the particular feature of the addition of the decay due to the contact of a storm with the continental mass. Therefore, this model generates better predictions if the storm interacts with the mainland. If the storm is relocated on the open sea, the Decay-SHIPS model and the SHIPS model provide approximately the same results.

Logistic Growth Equation Model Summary (LTCM)
This is a statistical model which uses the same input data as SHIPS, but its structure contains a simplified dynamic model, instead of a multiple regression model. Estimated intensity depends on potential maximum potential intensity, based on the ocean surface temperature.

3.5 Other models

HURASIM
This is a spatial simulation statistical model of the structure and movement of a hurricane, whose purpose is to reconstruct or estimate the force and direction of the wind during past storms. The model has been used to determine tables for the probability of damage for a number of exposure units (sites and ecosystems).

HURISK
This is essentially a statistical program with a graphic interface, which attempts to determine periods of recurrence of the wind and its routes, movements and intensities for coastal zones, or zones near the coast in the region.

3.6 Analytical model proposed

3.6.1 *General*

In order to make an appropriate quantification of future losses due to the passage of a hurricane through the region, modelling allows estimates to be made not only of the track of strong winds and pressure changes, but also of storm surges, and special rain regimes. This in turn, becomes a trigger for potential flooding and landslides throughout the zone of influence. With the direct allocation of a rain regime to the hurricane, periods of recurrence can be obtained for floods or the associated landslides

3.6.2 *Selection*

Given the current state of knowledge and the modelling for hurricane hazard, and the scope of results required for future application in the analysis of risk appraisal, a model was selected for stochastic storm generation using a statistical technique of preservation of historical hurricane tracks, which allows cyclones with characteristics statistically-compatible with historical items of the past, taking additional account of the fact that the

existing information on past storms at a sufficient level of detail for the correct application of the model.

3.6.3 *Analysis procedure*

Figure 3-1 presents a flow diagram with the principal elements of the hurricane hazard model applied. The main steps for the development of the hurricane has a model in the Central American area are the following:

(1) Generation of a set of stochastic events raised on historical information for the entire Atlantic basin. The set of events consists of thousands of tracks with defined parameters, such as intensity, size and shape, described at regular intervals throughout the tracks of those hurricanes. The average track and translational speed of the storm is identified, along with its distribution around these median values. Each event has its own frequency of occurrence. Specific past hurricanes were included within the set of events, in order to recalculate and calibrate losses and their effects.

(2) The stochastic events are generated by a simulation, using the random-walk technique. This method can be used to generate several thousand tracks. Each simulated track is different from each other simulated or historical track, but the set of simulated events maintains the same statistical properties as the set of historical events.

(3) Once the track has been defined, the intensity of central pressure is added, using another routine of random generation for each track. The frequency of storms by range of intensity and regions is calibrated against historical information and data. In order to complete the description of each similar should event, windfield intensity is added to each track, along with shape, using statistical relationships as a function of central pressure and latitude.

(4) The model for the generation of stochastic hurricane events simulates storms for the entire Atlantic basin, and the Central-Eastern Pacific. In considering hurricane hazard, the selection includes all hurricane tracks which could produce some impact on the country. This subset of events was verified to confirm that the tracks on their parameters were consistent with global frequency-severity relationships for the Atlantic, the South West Caribbean and the centre-East Pacific. At the same time, there was a check that severe, rare and special events have been included.

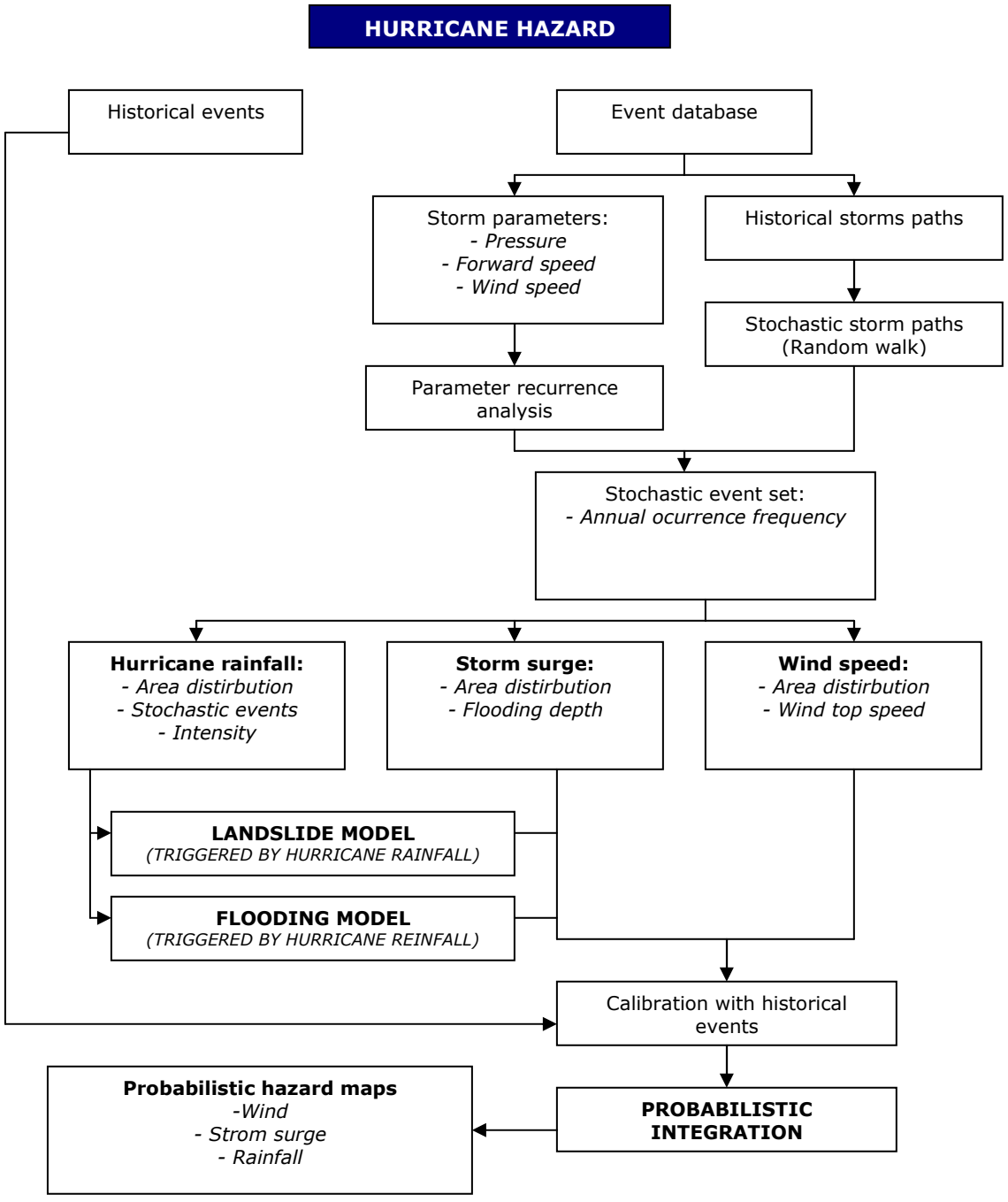

Figure 3-1
Flow diagram of the hurricane hazard model

(5) Wind velocity hazard maps were calculated and generated, together with associated levels of storm surge. For each point on the variable-resolution grid, the calculation

was made of expected peak squall velocity. A hazard maps were generated and produced for important historical events, along with at least five probabilistic maps which represents the intensity of wind velocity for period for return periods of between 10 and 1000 years. The model was calibrated and matched with parameters for the country.

(6) The information on tracks was converted to continental wind velocity, employing the following procedure:

(a) Definition of the wind gradient field (wind at a sufficient height above ground level not to reflect surface defects). The wind gradient at any point of interest is a function of the distance from the centre of the storm, the direction to the site relative to the track, central pressure, and the speed of advance of the storm, the relationship to a maximum wind, and parameters of the shape of the wind field.

(b) Use of surface rugosity and topography to calculate peak squall wind velocitys for five seconds at the site of interest.

This process is repeated for each time interval along the track, retaining the maximum windfall each location, and for the duration of the storm, a parameter which is then used to calculate losses.

(7) Tide calculations were made using the digital model for elevation which forms part of the bathymetry and topography of coastal zone Pressure and wind field for the storm at each time interval of basic data for numerical model of hydrodynamic flow were used to calculate the increase in sea level produced by the storm, and the resulting floods onshore.

(8) The intensity of rain associated with hurricanes. The model allows estimates to be made of the rainfall regime in the mainland, associated with the main parameters of each stochastic event.

(9) Calibration of the model, to ensure that the information is consistent with the statistical characteristics of the various parameters of the Atlantic zone, the southwestern Caribbean and the Central-Eastern Pacific. The return period for specific wind velocitys generated by the model were verified. At the same time, and to the extent allowed by information available, the general information related to storm surges and to intensity of rain was verified for mainland zones based on available historical information.

(10) Calculation and generation of rainfall regime hazards on the mainland, to be used as input data for flood and landslide hazard models.

3.6.4 *Hurricane simulations*

Records of hurricanes which have affected the region go back to the end of the 19th century. However, it was only in the middle of the 20th century the records began to be available of complete tracks, or of indicative parameters for severity, such as barometric pressure in the eye of the storm, or cyclostrophic velocity. In these circumstances, the useful database for hurricanes is limited, and it was necessary to extend it by generating (simulating) artificial hurricanes.

A method of perturbing the tracks of real hurricanes which have been correctly and fully recorded was used to generate artificial hurricanes.

In order to simulate the track of the artificial hurricane, it should be noted that its position must be established with geographical coordinates of longitude and latitude $x_s(t_k)$ and $y_s(t_k)$, respectively, at each point in time k. The process in relation should be conducted using the following expression, applicable to longitude, with a similar procedure for latitude:

$$x_s(t_{k+1}) = x_s(t_k) + \Delta X_{k,k+1} + e \qquad \textbf{(Ec. 15)}$$

where $x_s(t_{k+1})$ is the longitude at the moment $k+1$, $x_s(t_k)$ is longitude at the moment k, $\Delta X_{k,k+1}$ is the income and observed between k and $k+1$, and e is random variable with a zero medium normal distribution and standard deviation $\sigma = 0.5$. This deviation value is obtained on the basis of all hurricane is subject to perturbation, and a comparison of the results provided by the wind model data from all weather stations, given that there are there is no information to compare tide elevations. This assumes that if simulated hurricanes properly reproduce wind conditions, it can be expected that they may also be appropriate for storm surges.

3.6.5 *Wind modelling*

3.6.5.1 *Wind generated by hurricanes*

The determination of the maximum wind velocity at the site of interest associated with each hurricane uses a parametric wind volume is used, depending on the position of the eye of the hurricane, central pressure, P_0 [mb], , and the cyclostrophic radius, R (km). The first two parameters are to be found in weather bulletins. The cyclostrophic radius is calculated as:

$$R = 0.4785P_0 - 413.01 \qquad \textbf{(Ec. 16)}$$

Up to 1979, some meteorological reports admit central pressure. In the case of hurricanes were central pressure is not reported in the bulletins, the following equations were used for the calculation.

$$P_0 = 1019.08 - 0.182Vv - 0.0007175Vv^2 \quad \textbf{(Atlantic Ocean)} \qquad \textbf{(Ec. 17)}$$

$$P_0 = 1017.45 - 0.1437Vv - 0.00088Vv^2 \quad \textit{(Pacific Ocean)} \qquad \textbf{(Ec. 18)}$$

Where, Vv (kph) is the maximum sustained wind velocity, as recorded in weather bulletins. It is important to note that these relationships are only valid for central pressures higher than 888 mb.

The parametric model first calculates, for a hurricane in movement, the sustained wind velocity, averaged every eight minutes and V_m (kph) at the site of interest, located at a distance r (km) from the centre of the hurricane, evaluated at 10 m above sea level:

$$V_m = 0.886\left(F_v U_R + 0.5V_F \cos\left(\theta + \beta\right)\right) \qquad \textbf{(Ec. 19)}$$

Where V_F (kph) is the speed of displacement of the hurricane, $\theta + \beta$ is the angle formed by the direction of movement of the hurricane, and the point of interest at the distance r, U_R [kph] is the maximum wind gradient for a hurricane in a stationary state which is calculated as:

$$U_R = 21.8\sqrt{P_N - P_o} - 0.5fR \qquad \textbf{(Ec. 20)}$$

Where P_N. is normal pressure (1013 mb), and f is the Coriolis force parameter,

$$f = 2\omega \sin\phi \qquad \textbf{(Ec. 21)}$$

Where, $\omega \approx 0.2618\ rad/hr$ is the angular velocity of the earth, and φ is latitude,

$$Fv = Ur/U_R \qquad \textbf{(Ec. 22)}$$

is the buffer factor, or the ratio of wind velocity to the distance, with a maximum wind gradient (on the wall of the hurricane), and this is approximated using the following polynomial:

$$\log_{10}(F_V) = aX + bX^2 + cX^3 + dX^4 \qquad \textbf{(Ec. 23)}$$

Where

$$X = \log_{10}(r/R) \qquad \textbf{(Ec. 24)}$$

and *a, b, c* are coefficients obtained from Table 3-1 and are a function of *X* and of the Coriolis cyclostrophic number.

$$Nc = \frac{fR}{U_R} \qquad \textbf{(Ec. 25)}$$

Table 3-1
Parameters a, b, c for calculation of the expression (37)

	$X \le 0$	$X > 0$	
		$Nc \le 0.005$	$Nc > 0.005$
a	-0.233	$0.033 - 16.1Nc + 161.9Nc^2$	$-0.175 - 0.76Nc + 11.7Nc^2 - 28.1Nc^3 + 17Nc^4$
b	-12.91	$-0.43 + 38.9Nc - 316Nc^2$	$0.235 + 2.71Nc - 67.6Nc^2 + 189Nc^3 - 155Nc^4$
c	-19.38	$0.113 - 28.6Nc + 71.1Nc^2$	$-0.468 - 9Nc + 87.8Nc^2 - 224Nc^3 + 183Nc^4$
d	-8.311	$1.818Nc + 80.6Nc^2$	$0.082 + 3.33Nc - 26Nc^2 + 63.8Nc^3 - 51.4Nc^4$

The model described enables us to calculate wind velocity at 10m above sea level, averaged every eight minutes, and therefore corrections must be made to estimate average wind velocity every minute (V_c [kph]), as reported in weather bulletins. The following expressions were used:

$$V_c = 0.0012V_m^2 + 1.1114V_m \textbf{ (Océano Atlántico)} \qquad \textbf{(Ec. 26)}$$

$$V_c = 0.002V_m^2 + 0.9953V_m \textbf{ (Océano Pacífico)} \qquad \textbf{(Ec. 27)}$$

In order to take account of wind velocity variations over land, a calculation was made for an expression to reproducewind velocity recorded at weather stations (average every five seconds), based on wind velocity calculated with the parametric model. The expression obtained is the following:

$$Vv = Vc \ exp(-0.0043r) \qquad \textbf{(Ec. 28)}$$

In order to calculate wind velocity for a given site, taking account of the effect of friction with the surface of the ground and local topography, the following expression was as follows:

$$V = F_T F_\alpha Vv \qquad \textbf{(Ec. 29)}$$

Where F_T is the local topography factor indicated in table 3-2, and

$$F_\alpha = F_c F_{rz} \qquad \textbf{(Ec. 30)}$$

Is the factor which takes account of the size of the construction given by a zero (which varies between 0.9 and 1.0), and the variation with wind velocity with the altitude given by F_{rz}:.

$$Frz = 1.56 \left(\frac{10}{\delta}\right)^\alpha \quad si \quad Z \le 10$$

$$Frz = 1.56\left(\frac{Z}{\delta}\right)^{\alpha} \quad si \quad 10 < Z < \delta$$

(Ec. 31)

$$Frz = 1.56 \quad si \quad Z \geq \delta$$

Where Z (m) is the altitude at which we wish to determine wind velocity, α and δ are contants for the commonest types of terrain in the country, contained in Table 3-3

Table 3-2
Topography factor

Site	Topography	F_T
Protected	Closed valley	0.8
Flat	Flat terrain, open field, lack of important orographyc structures, slopes lower than 5%	1.0
Exposed	Hills or mountains, tarrain with slope higher tan 5%	1.2

Table 3-3
Values for α y δ for the commonest types of terrain in Central America

Type	Description	α	δ (m)
1	**Flat open ground** (open ground, almost flat without obstructions, for example flat coastal strips, swampland, airfields, pasture, and crops not surrounded by enclosures)	0.099	245
2	**Trees or standard construction** (crops or farms with two destructions, such as enclosures, trees and scattered constructions)	0.128	315
3	**Trees, residential district.** (land covered by a number of closely spaced obstructions, for example urban areas, suburbs, woodland. The size of constructions corresponds to housing)	0.156	390
4	**Many obstructions, city centre** (land with a number of large high buildings, closely spaced, such as in the centre of major cities and developed industrial complexes)	0.170	455

3.6.6 *Storm surges*

In order to determine the height of the water due to storm surges, η, the following simplified equation is used:

$$\eta = \frac{P_a}{100} + \frac{Kw^2 x}{g(h-\eta)} \ln\left(\frac{h}{\eta}\right)$$

(Ec. 32)

Where P_a [mb] (millibars) is the atmospheric pressure gradient at the evaluation point

(beach) with regard to normal pressure, x (km) is the distance between the wall of the hurricane and the site of interest (beach), W (m/s) is the normal component of wind velocity for the beach in m/s, g (m/s^2) is the acceleration of gravity, h(m) is the depth of the sea at the eye of the hurricane (if the depth is more than 200 m this is taken as a threshold value), and K is the air drag coefficient given by

$$K = \frac{\rho_{aire}}{\rho_{agua}} C_D \qquad \textbf{(Ec. 33)}$$

Where ρ_{aire} and ρ_{agua} are the relative specific weights of air and water, respectively, and C_D is a coefficient whose value is between $2x10^{-6}$ and $9x10^{-6}$ (for all hurricanes, $9x10^{-6}$ is used)

3.6.7 *Local rain*

This is expressed in terms of rainfall produced as a consequence of hurricane disturbance.

The following empirical expression is used to determine rainfall caused by each hurricane event:

$$P_{prom10\min} = FCv \cdot \left(\frac{122.15}{1 + 523.59 \cdot e^{-0.1412 \cdot R}} \right) \qquad si\ R \le 37km$$

$$P_{prom10\min} = FCv \cdot (36.52 - 34.40 \cdot e^{-2051.4 R^{-1.9193}}) \qquad si\ R > 37km \qquad \textbf{(Ec. 34)}$$

Where $P_{prom10min}$ [mm] is the average rainfall in 10 minutes, R (km) is the distance from the centre of the hurricane to the point of interest, and FCv is the correction factor which takes account of the intensity of the hurricane, through the wind velocity which is obtained as:

$$FCv = \frac{a}{(1 + e^{b - cv})^{1/d}} \qquad \textbf{(Ec. 35)}$$

Where v [m/s] is the maximum wind velocity of the hurricane, and parameters a, b, c and d are adjustment factors.

4 Evaluation model for intense rain hazard

4.1 Introduction

The analysis of rainfall and distribution of its intensity in a region analyse the first step for subsequent appraisals of a flood hazard, and eventually, as a detonating element for landslides. This chapter deals exclusively with the model for the generation of stochastic scenarios of rain intensity, consisting of information on record for a basin or region analyse. The flood hazard model is presented in Chapter 5 of this Report

4.2 Rain analysis

Rainfall at a given geographical point is a stochastic process with very variable frequency and intensity, depending on seasons. The basic parameters:

- Duration of the rain
- Average intensity
- Total volume
- Time between successive rainfalls

In terms of calculation, the most important value is the total rainfall volume P, which can be calculated by the equation $P = I \cdot t$ I is the average intensity and t is the total duration of the rain. These two parameters are not independent, since experiments show that the heavier the rain the shorter the duration, and vice versa.

4.2.1 *Intensity-duration-frequency curves (IDF)*

In the analysis of distribution of rainfall at a given point, in addition to the relationship between intensity and duration of storm (specific intensity-duration curves), the concept of probability or frequency must be introduced, in order to be able to make estimates for the future, with a quantitative evaluation of the hazard associated with rain, and an evaluation of risks to exposed infrastructure. This type of curve is commonly called the IDF curve, and has the following general form:

$$I(t,T) = at^b \qquad \textbf{(Ec. 36)}$$

Where I is the average maximum intensity of the storm, for a duration t, and a return period of T (millimetres/hour). The inverse of the return period is the rate of excedence, that is, the average frequency with which the intensity of the storm I is equalled or exceeded in each year ($1/T$.)

Parameters a and b are a function of the meteorological characteristics of the area, and must be estimated on the basis of experimental data.

The accumulated histogram appears as $H(t) = I(t,T) \cdot t = at^{b+1}$, and associated instantaneous intensity is $I(t) = dH(t)/dt = (b+1)at^{b}$.

4.2.2 *Curves for depth, area, duration, area , frequency curves*

These curves correspond to a particular representation at the level of a basin or sub-basin, of the characteristics of storms which have happened in the past. These curves relate to average rainfall over a given area with duration and frequency of occurrence of the storm, such that the area and depth of rainfall can be spatially projected.

These PADF curves are constructed on the basis of spatial IDF curve analysis, in relation to different seasons in the same basin, setting the duration of the storms and the frequency of occurrence.

4.3 Statistical models for rainfall estimates

Mathematical models that represent rainfall depend on a specified timescale. For long timescales, by the year or month, it can be assumed that self-correlation of rainfall does not exist, or can be ignored. In this case, it is enough to find a distribution of probability which can reproduce the variability of rainfall in the timescale considered.

We now describe some of the commonest models used in predicting rainfall:

4.3.1 *Hidden Markov models*

The hidden Markov Markov model (HMM) was first proposed by Rabena and Juang (1986) and subsequently modified by Hughes and Guttorp (1994) for use in climate-related studies. Hughes and Guttorp (1994) extended the HMM by including exogenous atmospheric factors to simulate rain, referring to a non--homogeneous Markov model (NHMM). The unifying characteristic between an HMM and a NHMM in the context of multivariable climate factors is based on the hypothesis that a non-observed state of the climate is related to certain observable patterns of spatial distribution on the ground (R. Merhotra, R. Sriakanthan, Ashish Sharma, 2006).

4.3.2 *Non-parametric model of the closest K-Neighbors*

With regard to the generation of rain events, the approach of the K-nearest neighbour (KN) takes account of sampling with the sampling of rainfall events at a number of locations, based on historical rainfall records. This implies the identification of days in historical records (nearest neighbours), which have similar characteristics to the previous day, and the use of observations of "today", as the basis for re-sampling. In order to simulate the timing, conditional re-sampling procedures by Markov were applied. The structure of spatial distribution of rainfall is maintained by simultaneous re-sampling in all stations (R. Merhotra, R. Sriakanthan, Ashish Sharma, 2006).

4.3.3 *Combination of daily and monthly series*

The stochastic generation of hydrological timeseries is a useful tool to design and manage systems of water resources. The complexity of models varies considerably, depending on the number of parameters. For many applications, it is important that the model may be able to reproduce key statistical characteristics not only on a daily basis, but also monthly and annually. This key statistical characteristics of the method consists first of generating to similar timeseries, one keeping the key statistical properties over a detailed timescale, and the other over a more ample timescale. The similarity between the two series is obtained using the fine-scale model as a basis for the model on the other scale, and using the same sequence of probabilities of non-excedence, for random elements and for input parameters for both models.

4.3.4 *Numerical weather prediction models NWP*

NWPs use complex computer programs, known as numerical forecast models, which processed data in supercomputers, and provide predictions of meteorological variables such as temperature, atmospheric pressure, wind, humidity and rainfall.

4.3.5 *DIT model for designed-rain prediction*

The DIT model is based on the dependence between intensity, duration, and recurrence of maximum rainfall, which are related through a logarithmic expression which includes the return period, and a persistence factor

4.3.6 *Artificial neuron networks ANN*

In recent years, ANN have become increasingly popular for hydrological forecasting, principally because of the wide range of application, and the ability to deal with non-linear problems. In the context of hydrological forecasting, results in some recent experiments indicate that ANN and can offer a promising alternative for the modelling of rainfall-run-off (Sedki, D Ouazar E., El Mazoudi, 2008), and other hydrological issues.

4.3.7 *Nowcasting*

This is a method to establish trends, involving the calculation of the velocity of high and low pressure in centres, fronts, cloud area and rainfall. The forecaster can use this information to predict where these characteristics can be expected at some future time.

4.4 The hydrological modelling of rain estimates

Taking the rain-run-off process as an example, there are three broad types of model:

- The empirical model, or the "black box" model (based on systems)
- The conceptual, quasi-physical model (based on dominant mechanisms)
- The physically-based distributed model (based on individual mechanisms)

Table 4-1
Hydrological models for estimates of rain

Model	Description	Calculation method	Input data	Results	References
Physically based model	Models based on continuum mechanics. Based on equations of motion of the constitutive processes, and solved numerically.	They include: ▪ Simple models: based on quasi-stationary states of hydraulic simulation. Flow in two directions: positive and negative ▪ Detailed Models: full simulation of the flow (eg Sipson). Based on the equation of Richard and St. Venant.	Historical climate data: temperature, precipitation, among others. Groundwater flow level data	Simple models: Levels of water for each node and discharges of water in certain connections. - Detailed models: Detailed attributes for the nodes.	**C. Makropoulos, D. Koutsoyiannis, M. Stanic, S. Djordjevic, D. Prodanovic, T. Dasic, S. Prohaska, Cˇ. Maksimovic, H. Wheater.** A Multi-Model approach to the simulation of large Scale karst flows
Conceptual model.	Based on observation. Determines which is the most appropriate structure to apply. Involves several specific parameters of the study area.	Simplified simulation, which studies the characteristics of the analyzed hydrosystem.	Historical climate data: temperature, precipitation, among others. Groundwater flow level data	Analyzed hydraulic system dynamics	**C. Makropoulos, D. Koutsoyiannis, M. Stanic, S. Djordjevic, D. Prodanovic, T. Dasic, S. Prohaska, Cˇ. Maksimovic, H. Wheater.** A Multi-Model approach to the simulation of large Scale karst flows
Black box model	Based on a pre-specified structure and basic components of the process.	Using transfer functions. Generation of results based on predefined rules of water distribution at different points.	Historical climate data: temperature, precipitation, among others. Groundwater flow level data	Out hydrographs	**C. Makropoulos, D. Koutsoyiannis, M. Stanic, S. Djordjevic, D. Prodanovic, T. Dasic, S. Prohaska, Cˇ. Maksimovic, H. Wheater.** A Multi-Model approach to the simulation of large Scale karst flows

4.5 Analytical model proposed

4.5.1 *General*

The proposal suggests the incorporation of a system of stochastic convective rain generation, which will allow definition of specific hazard scenarios for subsequent appraisal of the danger of associated flooding. The analysis model proposed comprises two principal phases: the formation of a database of rainfall events, and the spatial analysis of maximum rainfall.

4.5.2 *Selection*

The selection of the model for intensive rain takes account of the need to have a detailed model, whose results are based on the daily rainfall records, and whose application allows a characterisation of conditions of rainfall in basins and sub-basins, given their subsequent inclusion as an input into the flood hazard model.

The model selected allows a characterisation of rainfall conditions for a basin in terms of PADF curves, which relate the depth of expected rainfall within the area of influence, the duration of the storm, and the return period.

4.5.3 *Procedure for analysis*

Figure 4-1 gives a flow diagram of the model selected for evaluation of the hazard of intense rainfall. The principal steps for applying the model are as follows:

(1) *Characterisation of the basin analysed.* The basin must be characterised by an interplay of PADF curves. This characterisation is a preliminary step to the application of the model. However, Sections 4.5.4 and 4.5.5 present a procedure for defining it.

(2) *Geographical characterisation of the basin*. The model proposed must be operated at the level of a basin, and therefore, the limits or dividing lines of waters in it must be known.

(3) *Generation of stochastic storms*. Based on the information contained in the PADF curves, stochastic storms are generated with the random generation of location and shape (ellipsoid), with rainfall values which meet the depth-area ratio for a duration and frequency of occurrence defined.

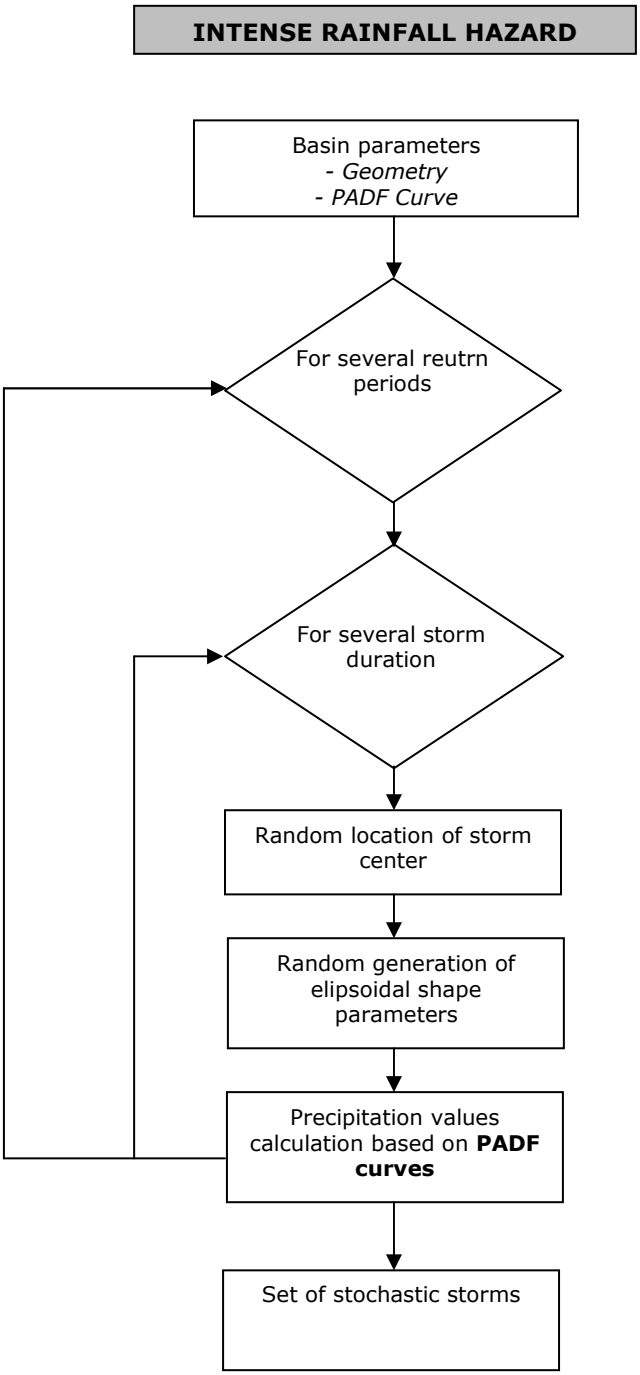

Figure 4-1
flow diagram of the intense rain hazard model

4.5.4 *Formation of a database for rainfall events*

This phase is designed to collect and store rainfall and graphic material required to develop the analysis of the succeeding phases. Criteria must be established to obtain information for this purpose, as follows:

1. Definition of areas of study. This is necessary in order to identify the stations for measuring and plotting rainfall within the areas, and on the periphery and in adjacent areas.

2. Identification of historical events of rainfall associated with hurricanes and other events due to intense rain caused by convective or low-pressure systems.

3. Historical records of the stations should be should have common and concurrent periods, to make the spatial analysis of maximum rainfall more robust. Information on rain measurement and thus plotting should be extracted from existing weather stations belonging to public and private organisations that measure rain.

4. Rain volumes should correspond to the daily records of rainfall, while information on plotting should be able to identify the mass curve of each rainfall event, and processing to determine maximum intensities for several durations. Rainfall plotting information should have a resolution in time of less than the daily resolution.

5. The storage of information should be made with computer tools in order to facilitate a suitable quality control for purposes of filtering, and subsequent complementation, easy to manage, and subsequent analysis in later phases.

4.5.5 *Spatial analysis of maximum rainfall*

The purpose of the model is to establish relations between the maximum depth of average rainfall (P), the area (A), in which this depth falls, duration (D.) during which rainfall occurs, and frequency (F) with which the event occurs with these characteristics of depth, spatial coverage and duration. This corresponds to curves of depth-area-duration-frequency. The PADF analysis determines the maximum volume of rainfall on areas of different sizes and for various durations of rain. The curves should be characteristic of the homogeneous areas mentioned above.

The method for the determination of PAD and PADF should be based on procedures proposed in literature, such as for example WMO (1969). The range of variation in areas should be established on the basis of isoyet maps generated for each available event, from the minimum specific equivalent value up to the maximum area covered by these events. Eventually, it may be necessary to extrapolate PAD and PADF curves for higher values than the historical maximum for the area. In relation to duration, we consider that these may range from 1 to approximately 10 days, by reason of rainfall associated with

hurricanes. In the same way that we consider the Gumbel distribution to be appropriate, we also consider that MPP is appropriate for spatial analysis of specific points.

The determination of rainfall data for analysis of PAD and PADF curves requires that dates be established for which one or more stations record significant depths, to be subsequently completed with records from the other stations. In this way, we can obtain the set of rainfall values recorded at all stations in a homogeneous same for each date data, which can then be produced in graphic form through isoyets, to establish the spatial distribution of rainfall on that date. Similar and additional analyses allow daily information to be detailed for shorter durations, as and when information on rain spread is available, and distributions in space and time could be established for each of these intervals. Equally, daily information can be added for greater durations, and the distribution in space and time can be established for each of the intervals. As a consequence, PAD curves can be constructed for significant events on all dates (one for each event and each duration), and on this basis, the analysis can made of frequency for several area values. The result of this is the PADF curve for the homogeneous hydrological zone.

The construction of a PAD curve in a hydrological a homogeneous zone will first require a definition of the duration, and then, isoyet maps can be compiled or generated for historical events in that duration. Next, each map is processed to identify the site or sites of highest rainfall, calculating average rainfall and measuring the related area covered. This is repeated successively, extending the coverage areas of the isoyets (progressively with values going from high to low), calculating average rainfall on the isoyets considered, and measuring the related areas. So, as the isoyet cover is expanded, average depth falls progressively, and the area increases, and this defines an inverse relationship between area and rainfall and intense rainfall events with spatial extension. The algorithm of the procedure is described as follows:

1 For each year, select events of intense rainfall with their spatial extension. Steps 2-16 relate to the analysis of events each year, with available information.

2 For each event, prepare an isoyet map for duration D, using computer tools. Stations which have not recorded rainfall should also be involved.

3 Identify the isoyets with the highest values. Let this highest rainfall value p_1 be $p1$, and let m_i be the number of isoyets with the value p_1.

4 Measure the areas enclosed in the isoyets with value p_1, and note these areas as a_i with i from 1 to m_1.

5 Estimate the average rainfall value at a_1, as $h_1 = p_1 + (p_{max} - p_1)/3$ J., is the specific maximum value of rainfall in the area a_1.

6 Add up the a_1 areas, that is: $A_1 = \sum_{i-1}^{m_1} a_1$

7 For the aggregate area A_1, calculate the average rainfall depth as:

$$H_1 = \frac{\sum_{i-1}^{m_1} h_{1i} a_{1i}}{A_1} \qquad \textbf{(Ec. 37)}$$

8 Identify the isoyet with a value immediately below $p_1$1, and this will be the value of p_2. Let this be the value of p_2 and let m_2 l be the number of isoyets with the value p_2.

9 Measure each of the internal areas with the isoyets with value p_2, let these areas be a_2.

10 Estimate the average rainfall value in a_2. as:

$$h_{2i} = \frac{h_{1i} a_{1i} + 0.5[p_2 + p_1][a_{2i} - a_{1i}]}{a_{2i}} \qquad \textbf{(Ec. 38)}$$

11 Add the a_2.areas, that is, $A_2 = \sum_{i-1}^{m_2} a_2$.

12 For the aggregate area A_2, calculate the depth of average rainfall as:

$$H_2 = \frac{\sum_{i-1}^{m_2} h_{2i} a_{2i}}{A_2} \qquad \textbf{(Ec. 39)}$$

13 Continue with the subsequent isoyet curves using a similar procedure. For the isoyet n, with a rainfall value p_n, and with enclosed areas a_n, estimate h_n as:

$$h_{ni} = \frac{h_{1i} \cdot a_{1i} + \sum_{j=2}^{n} 0.5[p_j + p_{j-1}][a_{ji} - a_{(j-1)i}]}{a_n} \qquad \textbf{(Ec. 40)}$$

14 Add up the a_n areas, that is, $A_n = \sum_{i-1}^{m_n} a_n$

15 For the aggregate area A_n, calculate average depth as:

$$H_n = \frac{\sum_{i-1}^{m_n} h_{ni} a_{ni}}{An} \qquad \textbf{(Ec. 41)}$$

16 Plot A_j vs. H_j.

17 Repeat the procedure described in steps 2- 16 for all rainfall events of duration D available for that year.

18 Superimpose the graph A_j vs H_j step 16 for all events of that year of duration D.

19 Establish the upper rainfall wrap for superimposing the previous step. The wrap represents the relationship between maximum rainfall and the special extension for

that year, and the PAD duration or curve. In that wrap, determine the maximum rainfall value for predetermined values in the area.

20 Repeat steps 2-19 for each of the other years available.

21 Form the annual series of maximum rainfall of duration D for each of the predetermined areas of step 19. Make a frequency analysis with this series, using the same probability distribution and the same method for estimating parameters applied in specific analyses.

22 Repeat steps 2-21 for other durations *D*.

23 With the result of a frequency analysis of steps 21 and 22, form the PADF curves.

As a result of the preceding analysis, we obtain the representative PADF curves for related homogeneous zones. Further, the analysis of the historical isoyet curves allows typical spatial distribution patterns to be established for rainfall events, which may be differentiated depending on origin - hurricane or intense rain. In complement to this, the preferred locations in these patterns in the area can be determined. The three ingredients mentioned (PADF curves, typical patterns, and preferred location) allow procedures to be established for the synthetic generation of rainfall events. For this, and in a controlled random exercise, the location of special rainfall events can be generated with characteristics, also controlled random, with the size and shape that meet the ratios contained in the PADF curves. The procedure is:

1 Select a set return period *T*.

2 Make a random determination of duration *D*.

3 Select area values in area *A*, within the range covered by the PADF curve and corresponding to duration *D* and frequency *T*.

4 Use the PADF curve to determine the maximum average depth value P_i

5 Effect a random generation of location, shape and size of the rainfall pattern.

6 Generate the related isoyet curves using the typical pattern, preserving the previous areas, related depths of rainfall Generate the related isoyet curves using the typical pattern, preserving the previous A_i areas, related depths of rainfall P_i

Table 4-2 shows the equations to prepare a circular or elliptical spatial pattern, because an ellipse is defined by the minor and major semi-axes *a* and *b* respectively, and one can be expressed as a function of the other as $b = Ka$. Table 4-2 contains the two columns for the values of areas and average maximum rainfall adopted from the PADF curve (steps 3 and 4), with the areas arranged from smaller to larger. The third column shows the equations to determine the value related to the isoyet of the elliptical pattern. Columns 4 and 5 allow calculation of values for each isoyet of the major and minor semi-axes.

Table 4-2
Determination of spatial synthetic patterns

A_i	P_i	Countour value, h_i	Minor axis a_i	Major axis b_i
A_1	P_1	$h_1 = P_1$	$a_1 = \left(\frac{A_1}{\pi K}\right)^{0.5}$	$b_1 = Ka_1$
A_2	P_2	$h_2 = \frac{2(P_2A_2 - P_1A_1)}{A_2 - A_1} - h_1$	$a_2 = \left(\frac{A_2}{\pi K}\right)^{0.5}$	$b_2 = Ka_2$
A_3	P_3	$h_3 = \frac{2(P_3A_3 - P_2A_2)}{A_3 - A_2} - h_2$	$a_3 = \left(\frac{A_3}{\pi K}\right)^{0.5}$	$b_3 = Ka_3$
…	…	…	…	…
A_n	P_n	$h_n = \frac{2(P_nA_n - P_{n-1}A_{n-1})}{A_n - A_{n-1}} - h_{n-1}$	$a_n = \left(\frac{A_n}{\pi K}\right)^{0.5}$	$b_n = Ka_n$

5 Evaluation model for flood hazard

5.1 Introduction

In particular, the risk of flooding due to the overflowing of rivers after excess rain is directly related to rainfall in the basin analyzed, and the topographic characteristics of the terrain surrounding the watercourse. Therefore, models used to determine run-off based on rainfall causing it, are based on run-off ratios. The method for estimating the risk of flooding is divided into a hydrological analysis, hydraulic analysis, and a plane flow analysis.

a) Hydrological analysis
A hydrological analysis determines the relationship between rainfall falling in an area with the quantity of water which runs off towards watercourses, and if the latter is excessive, produces flooding.

b) Hydraulic analysis
A freshet is defined as a change suffered by the flow of a watercourse from one transverse section to another, located after a stretch of the river or a dam. The change may be one of form, or displacement over time. The freshet must be produced by flow simulation models for natural watercourses and plain flow models. This model requires detailed information on affluents into the watercourses, slopes, and characteristics of their sections.

c) Analysis of plain flooding
The dynamic character of flood and the influence of the displacement of water towards lower areas makes it necessary to use mathematical models which at least include two-way horizontal flow equations based on equations for the conservation of the quantity of movement and continuity. This model requires information on the overflow, and detailed topography of the zone studied.

The field of modelling of hydraulic phenomena is in some way similar to the modelling of hydrology: there is no model which can hydraulically represent all watercourses. Therefore, the modeller must use appropriate judgement so that, based on the particular characteristics of the problem and the characteristics of the information available, he can select the most appropriate model.

The analysis of flows in rivers and in open channels is generally based on physics; however, there are models which are not. There are three main types of hydraulic models:

- Physics-based hydrodynamic models
- Stochastic models
- Conceptual models

5.2 Analytical model proposed

5.2.1 *General*

Flood hazard is expressed through a geographically distributed measurement of intensity, which in turn is linked to the probability of its recurrence. Intensity can be defined as a function of depth and water velocity, and the duration of a freshet. Therefore, the definition of flood hazard (as a function of potential damage) should take account of the probability or frequency of accounts of the freshet, and levels or heights of the head of water. It is also possible in particular cases to consider the maximum specific water velocity as a complementary measurement of intensity.

5.2.2 *Selection of the model*

This analysis attempts to differentiate between floods produced by rain related to hurricanes, and floods produced by rain regimes not associated with hurricanes. In this way, a probabilistic estimate can be made of the loss associated with hurricanes in a comprehensive manner, including not only losses associated with strong winds, but also losses from storm surge and floods and landslides associated with an increase in the rain regime. It also allows a probabilistic assessment to be made of losses associated only with floods, regardless of the origin of the rains that produce them.

The principal result of a flood hazard model is the demarcation of areas subject to flooding for a defined return period or rate of excedence. The determination of areas prone to flooding requires knowledge of historical events, a detailed model of elevation of the terrain, data of discharge flows in the basins of the principal rivers, and geometrical data of a given number of transverse sections down the course of the river in the flood basin.

For this study, the approach selected was that of a hazard using a probabilistic procedure to combine the following components:

- A stochastic set of rainfall events, in which one event is defined as a spatial distribution of intensity and duration of the rain.

- A flood model, which defines a spatial extension of floodable areas for different levels of rain intensity.

With this approach, two flood hazard models were chosen, with different levels of resolution in the analysis. The first is a simplified model of a parametric nature, which allows an estimate to made of regions prone to flooding throughout the country, under the effect of different stochastic storms. The second is a detailed model, which allows a determination of the extent of flooding around a watercourse, based on rainfall produced by simulated storms.

5.2.3 *Analysis procedure*

Figure 5-1 shows the flow diagram of the model for flood hazard. The main steps for the development of the flood hazard model in the zone selected are the following:

(1) *Generation of a set of stochastic rain events*. Using the models for the generation of the rain events, associated with hurricanes and otherwise, (Chapters 3 and 4, respectively), a set of stochastic scenarios for rainfall is generated, which are consistent with the regional characteristics of occurrence of rain. These events are used as input data for the hydrological model, in order to determine the average flow of the main rivers in zones affected.

(2) Determination of parameters for rain. Intensity of rain and its duration will be determined on the basis of the scenarios generated, in order to determine the portion of total rainfall which may run off and arrive in natural watercourses or floodable areas.

(3) *Flood modelling*. Using the available information and the scope of analysis to be made, there is a choice of flood model to be made in order to obtain the best possible results. The models for analysis is such developed are detailed in the sections that follow.

(4) *Integration of the hazard*. In applying the model for each of the rain scenarios defined, a set of stochastic flood scenarios is constructed, each of which has an annual frequency of occurrence equal to that of the detonating scenario. This set of scenarios is representative of all flood events which may happen in the region. At this point, the flood hazard may be included, in order to obtain the rates of excedence for different values of intensity, and maps for the same return period.

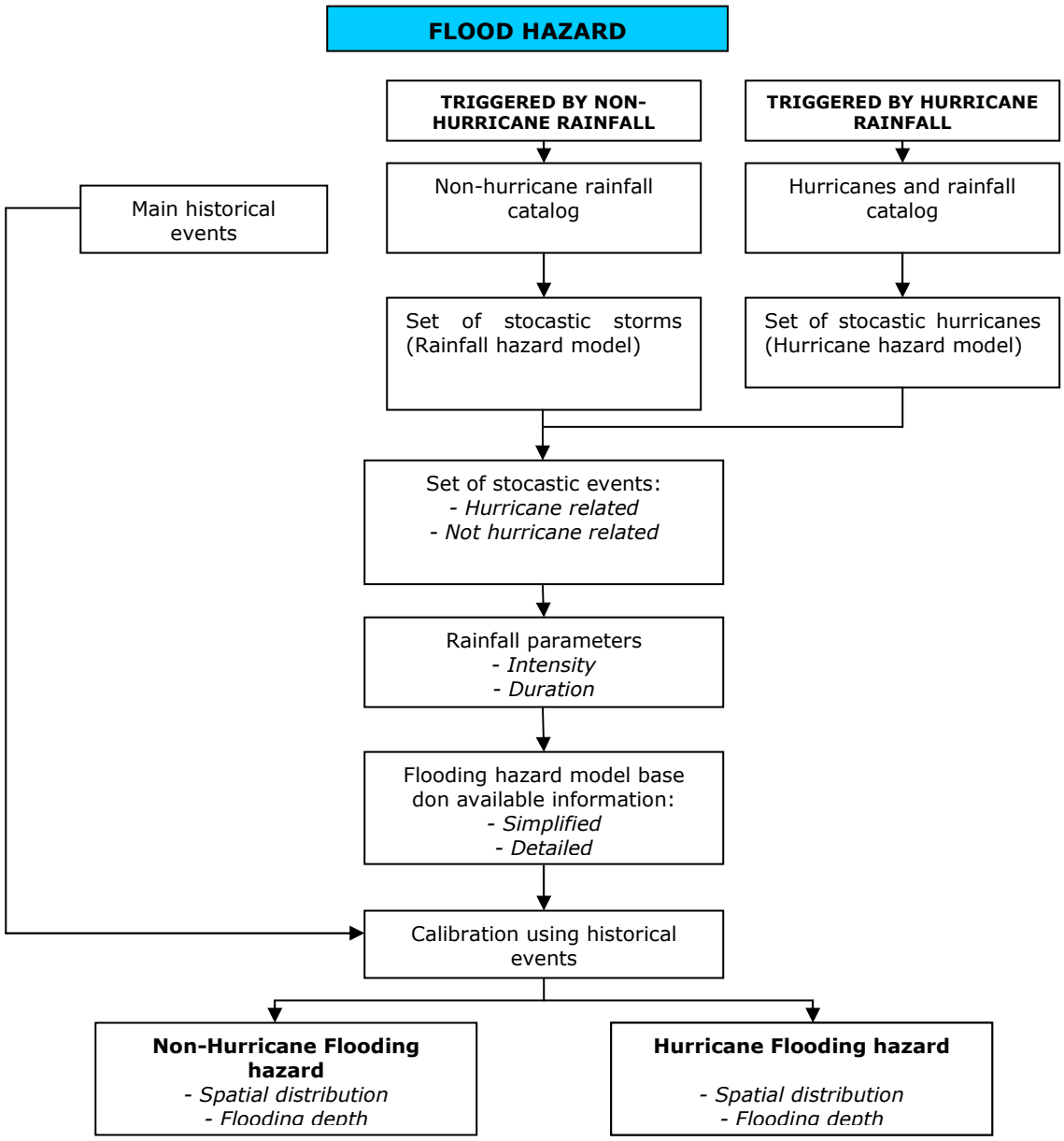

Figure 5-1
Flow diagram of the flood hazard model

5.2.4 *Simplified analysis of floods*

The intensity of rain must be translated into an effective depth of rainfall, which corresponds to the portion of total rainfall which may run off and reach natural watercourses or floodable areas. The percentage of total rainfall which then becomes effective depends mainly on the characteristics of saturation and permeability of surface soils, vegetation cover, and use.

The depth of flooding is obtained based on effective rainfall, employing flooding factors, which characterise the territory of a given region, in terms of how potentially floodable they are, as a function of topography and nearby slopes.

5.2.4.1 *Estimate of effective rainfall*

Effective rainfall corresponds to the intensity of residual rain, after a portion of the total depth of rainfall provided by the storm has been dissipated by hydrological processes of infiltration and evapotranspiration. The run-off is calculated as a function of the total value of rainfall, and the run-off number at a given point, using Chow´s expression (1994):

$$P_e = \frac{\left[P_m - \frac{508}{N} + 5.08\right]^2}{P_m + \frac{2032}{N} - 20.32} \qquad \textbf{(Ec. 42)}$$

Where P_e is the effective rainfall in centimetres, P_m is the rainfall from the storm in centimetres, and N is the run-off number.

The run-off number is the global indicator of the amount of water which will be absorbed or transpired by surface soils. It is obtained as a function of the use of the land, vegetation cover and conditions of infiltration and transpiration of the surface soil. Table 5-1 shows values of N for different soils and conditions of use.

The range of application of equation 58, according to Ven T Chow is for values of:

$$P_m > \frac{508}{N} + 5.08 \qquad \textbf{(Ec. 43)}$$

Outside this interval, it is considered that effective rainfall is equal to zero. Also, the check must be made that effective rainfall is not greater than storm rainfall.

Table 5-1
Values of N for different types of soil and land uses (cover)

LAND USE OR COVER	SURFACE CONDITION	SOIL TYPE			
		A	B	C	D
Forests (seeded or cultivated)	Sparse, low transpiration	45	66	77	83
	Normal, intermediate transpiration	36	60	73	79
	Thick or high transpiration	25	55	70	77
Roads	Unpaved	72	82	87	89
	Paved	74	84	90	92
Natural forest	Highly sparse or low transpiration	56	75	86	91
	Sparse, low transpiration	46	68	78	84
	Normal, intermediate transpiration	36	60	70	76
	Thick or high transpiration	26	52	62	69
	Highly thick, high transpiration	15	44	54	61
Rest (uncultivated)	Straight furrows	77	86	91	94
Cropped furrows	Straight furrows	70	80	87	90
	Contour-furrows	67	77	83	87
	Terraces	64	73	79	82
Cereals	Straight furrows	64	76	84	88
	Contour-furrows	62	74	82	85
	Terraces	60	71	79	82
Leguminous (mechanically or manually scattered) or pasture rotation	Straight furrows	62	75	83	87
	Contour-furrows	60	72	81	84
	Terraces	57	70	78	82
Rangeland	Poor	68	79	86	89
	Normal	49	69	79	84
	Good	39	61	74	80
	Contour-furrows, poor	47	67	81	88
	Contour-furrows, normal	25	59	75	83
	Contour-furrows, good	6	35	70	79
Pasture (permanent)	Normal	30	58	71	78
Impermeable surface		100	100	100	100
SOIL CLASSIFICATION (regarding its influence in the material when runoff)					
Type A: (Minimum runoff). Includes gravel and medium size sands, clean and mixed.					
Type B: Includes fine sands, organic and inorganic, limestone and sand mixtures.					
Type C: Very fine sand, low plasticity clay, mixtures of sand,limestone and clay.					
Type D: (Maximum runoff). Mainly including high plasticity clay, shallow soil with nearly impermeable subhorizons close to the surface.					

5.2.4.2 *Flooding factors*

The depth of the flood is calculated based on effective rainfall and flooding factors, which mainly depend on the topographical conditions of the area under study. The flooding factors assess the potential of a particular point to be flooded. In Figure 5-2 illustrates the flooding factors for this particular zone.

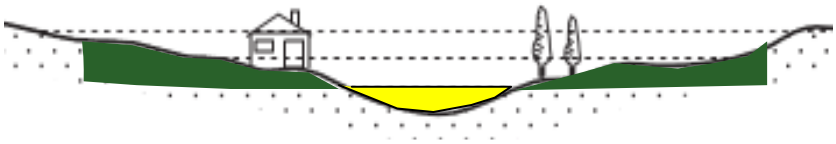

Figure 5-2
Figure exemplifying regions of expansion in low areas

For the definitions of these factors, we can differentiate four zones of interest:

1) Low areas, or area surrounded by mountains, with a greater risk of flooding, which are similar in shape to watercourses. These zones are highlighted in Figure 5-2 in yellow. The flood flow is equal to the effective rainfall, plus 50%.
2) Sites close to areas identified as watercourses. The flood flow is equal to the effective rainfall plus 20%. These zones are highlighted in Figure 5-2 in green.
3) Sites with low or flat topographical slope. It is considered that the flood flow is equal to the effective rainfall.
4) In places with high topographical slopes, it is considered that no flooding will occur.

Based on effective rainfall and flood factors, an approximate estimate is made of the value of the depth of flooding, giving general consideration to the type and use of soil, and topographic conditions.

5.2.5 *Detailed analysis of floods*

This model employs a method which involves the three most important processes in estimating flood hazard: *hydrological analysis, hydraulic analysis, and plain floods*.

5.2.5.1 *Hydrological analysis*

The flow for each the flood scenario is determined by using the information from the basin under study, demarcating the main watercourse, and applying rainfall information, different types of run-off in the region, and the general topography of the basin. The procedure for analysis is the following:

1. With the net rainfall information for each the rain scenario, the effective rainfall

within the basin is obtained, using the Chow equation for the simplified method (Equation 50), and with the N factors for run-off for the basin analysed.
2. Effective rainfall in the basin is then added up to obtain the total volume of run-off
3. The triangular unitary hydrogram method is used to determine flows, with some adaptations to consider the volume of run-off.
4. With each scenario and characteristics of the unitary hydrogram, we can obtain the correct run-off hydrograms for each event, considering the form of the unitary hydrogram with the loss from the event analysed.

5.2.5.2 *Hydraulic analysis, and plain flooding*

The data from the run-off hydrogram for each event are required for hydraulic analysis and plain flooding, and the zone analyzed must be demarcated. There must be detailed topography to include the principal characteristics of the watercourse and floodplains with sufficient resolution. The quality of the results will depend on the quality of this topography, and it is therefore very important to have the best possible resolution for the region of interest.

The steps for the application of the process of hydraulic analysis and plain flooding are the following:

1. A point is selected as the basis for conducting the analysis. It should be a point on a watercourse close to a settlement of interest, or the mouth of the basin affected.
2. With detailed topography, and the hydrogram for each event, a two-dimensional flow algorithm is applied, and the algorithm analyses each cell of the topography at several instants of time.
3. Maximum flood values for each event are stored, and this creates a flooding grid per event.

In this procedure, for the sake of simplicity, the triangular unitary hydrogram method has been chosen (Figure 5-3), to characterise the hydrograms of the entry of water into the watercourse analysed. The physiographic characteristics of the basin must be known in order to do so.

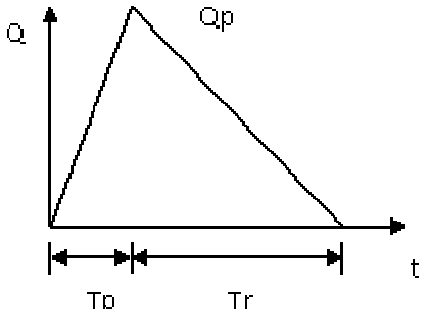

Figure 5-3
Triangular unitary hydrogram model

The peak flood flow is estimated as:

$$Q_p = 0.566 \frac{hpe\,A}{nTp} \qquad \textbf{(Ec. 44)}$$

Where,

$$Tp = \frac{Tc}{2} + 0.6Tc \qquad \text{For small basins} \qquad \textbf{(Ec. 45)}$$

$$Tp = \sqrt{Tc} + 0.6Tc \qquad \text{For large basins} \qquad \textbf{(Ec. 46)}$$

$$n = 2 + \frac{A - 250}{1583.3} \qquad \text{For basins where A<= 250 km}^2 \text{ then n= 2.0} \qquad \textbf{(Ec. 47)}$$

$$Tb = n\,Tp \;\; ; \;\; Tb = Tp + Tr \qquad \textbf{(Ec. 48)}$$

Where *hpe* is the effective layer of water in millimetres, *A* is the area of the basin in square kilometres, *Tc* is the time of concentration in hours, *Tp* is the peak time in hours, *Tr* is the lag time in hours, *Tb* is the base time in hours, and *n* is the correction factor for the area.

The direct run-off hydrograms are calculated multiplying each of the ordinance of the trainer unitary hydrogram by the effective rain, hpe), expressed in millimetres

The time of concentration to can be calculated applying Kirpich´s equation, expressed as:

$$t_c = 0.0003245 \left[\frac{L}{\sqrt{S}} \right]^{0.77} \qquad \textbf{(Ec. 49)}$$

In which t_c is the time of concentration in hours, *L* is the length of the principal watercourse in m, and *S* is the average slope of the main watercourse.

With the information on the watercourse and general topography, we obtain the average slope of the watercourse implying the Taylor-Schwantz (Springal, 1970) method, with:

$$S = \left[\frac{L}{\frac{l_1}{\sqrt{S_1}} + \frac{l_2}{\sqrt{S_2}} + \ldots + \frac{l_n}{\sqrt{S_n}}} \right]^2 \qquad \textbf{(Ec. 50)}$$

Where the length of the main watercourse *L* is divided into in number of segments of length *l*, and the slope *S* is calculated for each.

5.2.5.3 *Mathematical model of two-dimensional flow*

The dynamic character of floods, and the influence of the displacement of water towards lower areas makes it necessary to use mathematical models which are least include two-way horizontal flow equations. The method proposed considers a two-dimensional numerical model based on the equation from the conservation of quantity of movement, and in the continuity equation. Here, the velocities correspond to an average vertical value. The flow is considered for a region with or without water.

The dynamic equations which describe the *conservation of the quantity of movement* are*:*

$$\frac{1}{g}\frac{\partial u}{\partial t}+u\frac{\partial u}{\partial x}+v\frac{\partial u}{\partial y}+\frac{n^2|u|u}{h^{\frac{4}{3}}}=-\frac{\partial h}{\partial x}-\frac{\partial z}{\partial x} \qquad \textbf{(Ec. 51)}$$

$$\frac{1}{g}\frac{\partial v}{\partial t}+u\frac{\partial v}{\partial x}+v\frac{\partial v}{\partial y}+\frac{n^2|v|v}{h^{\frac{4}{3}}}=-\frac{\partial h}{\partial y}-\frac{\partial z}{\partial y} \qquad \textbf{(Ec. 52)}$$

in which u and v are the components of velocity in directions x and y respectively, in is the coefficient of velocity according to Manning´s formula, h is the level of water-free surface with respect to the level of natural terrain, and t is time.

The principle of the conservation of mass (*continuity equation*) in two horizontal dimensions establishes that:

$$\frac{\partial h}{\partial t}+\frac{\partial}{\partial x}uh+\frac{\partial}{\partial y}vh=0 \qquad \textbf{(Ec. 53)}$$

The area (in horizontal projection) of the plain to be flooded is divided into cells of a rectangular shape, the Δx-long and Δy wide. In order to calculate the water flow in a flood plain, a system of differential equations must be solved, performed by the above equations and considering such an initial and frontier conditions.

Given the detailed characteristics of this method of analysis, we recommend that a thorough review be made of information before it is applied, since it is a process which demands a considerable amount of computer time.

6 Evaluation model for landslide hazard

6.1 Introduction

It is common in engineering practice to define the stability of a mountainside in terms of the safety factor, obtained from a mathematical analysis of stability. However, not all factors which affect stability of a slope can be quantified for inclusion in a mathematical model. Therefore, there are situations in which a particular approach does not produce satisfactory results. Despite the weaknesses of a simplified model, if the safety factor can be determined assuming probable fault-prone surfaces, the result will be information which is very useful for decision taking.

6.1.1 *Limit of equilibrium and safety factor*

Limit of equilibrium methods are based on the supposition or discovery of a fault surface, in which there are critical conditions of stability which may be characterised by a safety factor. This type of analysis requires information on soil resistance, but does not generally require information on the stress-deformation ratio. The equilibrium limit system supposes that in the case of a force, the actuating and resistant forces on it are equal along the entire fault surface, and equivalent to a safety factor of 1.0.

The safety factor is employed to discover what the hazard factor is, in the face of a possible fault in a slope, in the worst conditions of comportment for which it is designed. Fellenius (1972) presented the safety factor as a ratio calculated between the real shear resistance of slopes, and critical shear stress which tries to produce a rupture along the supposed surface.

$$FS = \frac{Shear\ strength}{Shear\ stress} \qquad \textbf{(Ec. 54)}$$

In circular surfaces, where there is a turning centre and resistant and actuating moment, the expression is as follows.

$$FS = \frac{\mathrm{Re}\,sisting\ moment}{Acting\ moment} \qquad \textbf{(Ec. 55)}$$

6.2 Analytical model proposed

6.2.1 *General*

The principal objective of a probabilistic analysis of the hazard is to provide the necessary information on hazards, in order to make a reliable calculation of the various probabilistic parameters related to loss, and the effects of different natural phenomena, for different return periods. The return period for the analysis is in general linked to the return period of

the detonating phenomenon, in this case, an earthquake.

As a basic parameter of hazard intensity, a selection has been made of the inverse of the safety factor, which we will refer to as the "unsafety factor". We do so, in order to have a parameter which will grow with the level of the landslide hazard obtained.

This method allows the estimated loss from landslides to be grouped together with the general set of events associated with landslides, regardless of the detonating event, or losses associated with a specific events, in which case we also obtain not only the losses associated with landslides, but also the movement of the ground, and other information.

6.2.2 *Selection*

Given the complexity of the phenomenon of slope instability, there are a number of existing methods to evaluate susceptibility, heterogeneity of the phenomenon in respect of types of faults or rupture, and the difficulty in obtaining detailed information for the characterisation of conditions which will induce the phenomenon, and four models for hazard evaluation were selected, each applicable to different levels of resolution of the information. The models selected are widely accepted by the international scientific community, and represent the state of the art in the evaluation of the likelihood of landslides.

6.2.3 *Procedure for analysis*

Figure 6-1 shows a flow diagram of the landslide analysis model. The method proposed includes the following main steps:

(1) Formation and adaptation of all information required, including topographical information based on the Digital Elevation Model (DEM), and geological and geomorphological information, information on soils, land use, water tables or groundwater, soil cover, etc.

(2) Selection of critical areas as a function of the density of events in the past, and according to geological and geotechnical susceptibilities. The main factors to be taken into account for zoning are the following:

- Evidence of past landslides.
- Presence of clay and lutite rock, with the development of weathering profiles parallel to the terrain, and local weathering profiles at greater depths in some new lutite units (rotational fault).
- Existence of harder rock (sandstone, conglomerate), from the Cretaceous and Tertiary periods for example, which will present mechanisms for a rupture dominated by structural configuration (diaclases, down dips). This mechanism may also appear in lutites or arcillolites with down dips.
- Presence of colluvial deposits which may originate rotational faults, and also plane faults in contact with rock.
- Primary detonating factors, such as the effect of sheer on stretches of road, the

action of water, and erosion/undermining.

- Evidence of effects of intensive deforestation, and excessive overload on the crown of slopes.
- Additional characteristics of the geological formations found.
- Map of topographic slopes.

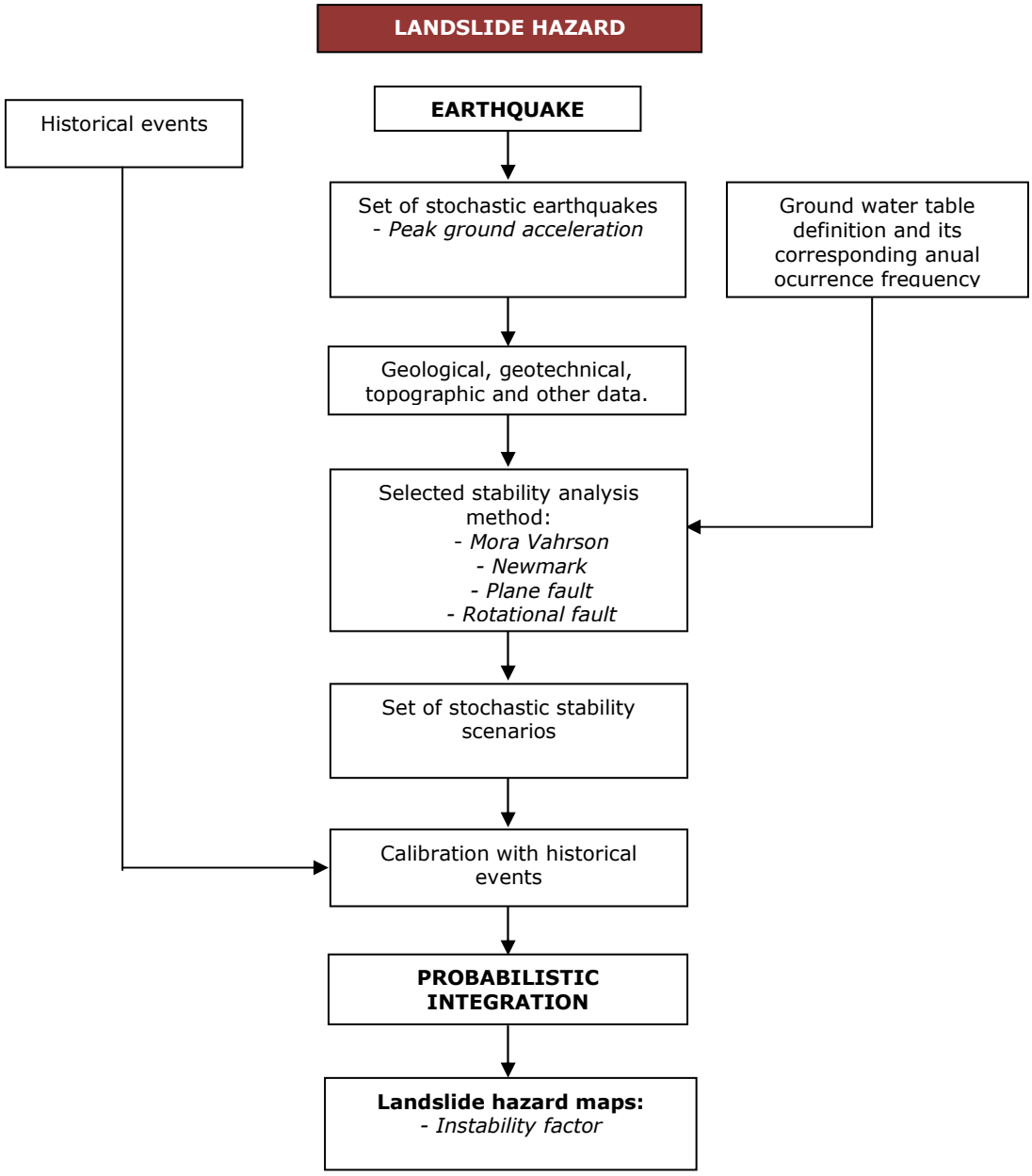

Figure 6-1
Flow diagram for the model of landslide hazard.

(3) Evaluation of susceptibility to landslides. Taking account of the high heterogeneity of materials, topographical conditions, vegetation cover and types of rupture in hillsides,

four different evaluation methods are proposed for stability, such that it would be possible to apply that which best describes the condition of the expected conditions of landslide to each case. The methods proposed are:

- Mora Vahrson
- Newmark
- Plane faults
- Detailed rotational fault

Each of these methods requires a different level of detail with regard to input information. When the model best suited to the conditions of the region analysed has been selected, and with available information, the application of the model requires the following steps:

- Selection of humidity conditions (water table), and annual frequencies of occurrence
- Selection of a set of stochastic seismic detonating events, calculated on the basis of seismic hazard conditions.
- Evaluation of susceptibility to landslide in the area under study, for different detonating events and for conditions of the height of the water table selected
- Generation of a set of stochastic landslide scenarios, based on a set of defined detonating scenarios, expressing the hazard in terms of the safety factor.

(4) Each of the landslide events, defined on the safety factor maps, or maps of susceptibility to landslide, has a given level of probability for the related detonating event, or equivalent frequency of occurrence.

6.2.4 *Susceptibility to landslide*

We will now describe the methods suited to the calculation of stability proposed. These methods have different scopes, and require different levels of detail for information inputs.

6.2.4.1 *Mora-Vahrson method (1993)*

This method[2] can be defined as a heuristic method, which uses more morphodynamic indicators for which information can generally be simple to find. If this method is used, the results obtained will depend on the indicators known as *susceptibility factors*, such as the topography of the site, the lithological conditions and the natural humidity of the soil, and also take account of other known indicators such as detonating factors and seismic intensity. The indicators mentioned are combined in accordance with a specific weighting, which defines their degree of influence in obtaining a relative hazard value for landslides.

In order to determine the hazard by this method, five morphodymanic indicators are used,

[2] See references at the end of the document

and these are grouped into two categories, which were defined above, namely, the susceptibility parameter, and the trigger parameter.

The combination of relative weights of these parameters is affected by the following equation:

$$Ad = Susc \cdot Disp \qquad \textbf{(Ec. 56)}$$

Where A_d is the landslide hazard, *Susc* is the susceptibility parameter, and *Disp* is the trigger parameter.

It should be mentioned that the parameter of susceptibility is defined as a combination of parameters of lithology, ground slope, and soil humidity, with the following expression:

$$Susc = Rr \cdot L \cdot H \qquad \textbf{(Ec. 57)}$$

Where *Rr* is the index of influence of relative relief, *L* is the index of influence of lithological conditions, and *H* is the index of soil humidity.

If the intention is to measure susceptibility of a landslide caused by the earthquake, the trigger parameter is defined by the maximum seismic intensity *S*. Therefore, the expression to define the landslide hazard from slopes detonated by an earthquake can be expressed as follows:

$$Ad = \left(Rr \cdot L \cdot H\right) \cdot S \qquad \textbf{(Ec. 58)}$$

The weighting assigned to each of the indices involved in Equation 64 is defined in Mora and Vahrson (1993). From this equation, the indicator that measures ground velocity, Rr measures rugosity as the difference between the maximum and minimum elevations found in an area of one square kilometre.

It must be remembered that the results obtained by this method are qualitative, and only indicate conditions of relativity in comparison to the adjacent situations in other areas.

6.2.4.2 *Plane fault method*

This method is applicable to translational landslides, with particular morphological characteristics which allow modelling as an infinite slope. In a translational landslide, the mass of material is displaced downwards, along a more or less flat or slightly undulating surface, and that there is very little or no rotation or turning. A rotation movement tries to stabilize itself, while a translational movement may progress indefinitely down the hillside.

Translational movements are frequent in rocky areas affected by discontinuities, such as fractures, folds or schists, with an orientation relatively parallel to the slope, and on hillsides which have a considerable soil thickness or detritus in contact with a less altered.

This condition, though not unique, is common in many real cases, where an unweathered layer of soil or rock overlies more competent strata, creating a contact surface which acts as a surface over which other materials may slide. In many translational landslides, the mass is deformed, or breaks up, and may become a flow.

Keefer (1984, 2002) analyzes seismic data around the world, and concludes that most processes of movement associated consist of translational landslides, break up into fragile materials, slippage of rocks, and rock faults. Further, most detritus flows start as surface or deep translational landslides, and subsequently undergo processes of liquation, as they advance down the slope (Gabet and Mudd, 2006).

Therefore, the method presented here refers to translational landslides, and it is assumed that the volume mobilised turns into a flow of detritus, which is a type of process that is considered to be among the most destructive, and which has caused many deaths in several parts of the world (Alexander, 1989; Scout *et al.*2005; Caballero *et al*, 2006).

The method of analysis of the stability of an infinite slope (Taylor, 1948) has been widely used in technical literature for regional zoning of danger and risk (Van Westen and Terlien, 1996; Jibson *et al*, 20090;Luzi *et a*l, 2000;Alcántara-Ayala, 2004). This is so because of the simplicity of the method, its easy integration into a GIS, and the fact that on a regional scale it is almost impossible to use more accurate methods, given the lack of geotechnical data and ignorance of the precise mechanisms of movement (Luzi *et al*, 2000.).

In the conditions in which a fault is produced parallel to the surface of the slope, at a given depth, and the fault is long compared to its thickness, the analysis of the infinite slope can be used in approximate form (Figure 6-2). It is a very quick and simple method of calculation, supposing a long slope with a layer of soil, detritus or rock, in which any size of column of material is representative of the entire slope.

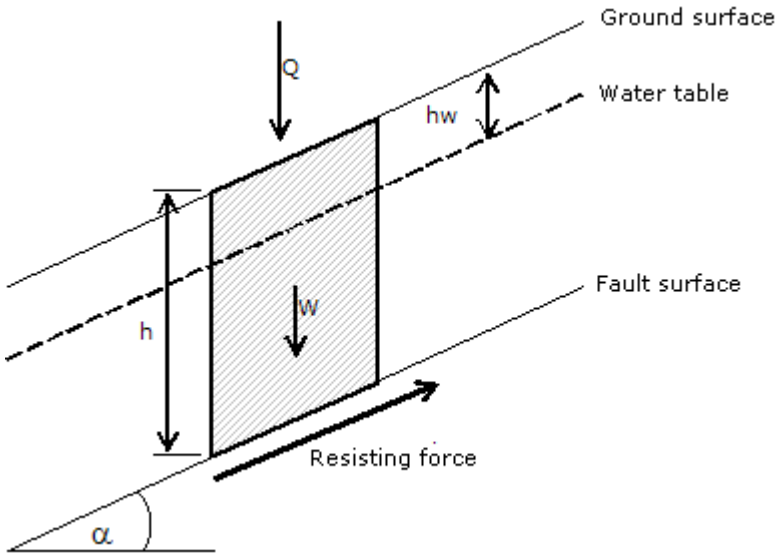

Figure 6-2
Simplified scheme of the method of the infinite slope

The calculation is made through a cell-by-cell analysis, calculating the relationship between actuating and resisting forces along the fault plane. The calculation ignores the effect of horizontal force between slices, which is approximately annulled between one slice and the next.

The terms which form part of the calculations are:

1. The height of the first stratum that defines the landslide plane, and which is determined by geotechnical information obtained;

2. Cohesion between strata, also defined by geotechnical information;

3. The cosine and a sine of the annual of the surface to the horizontal, which depends on topography; and

4. Seismic separation, described by iso-acceleration curves, according to the seismic hazard.

The expressions for the calculation of the safety factor by the plane fault method are:

$$Fh = \gamma.l.b.h \qquad \textbf{(Ec. 59)}$$

Which can also be expressed as

$$Fh = W.K / g \qquad \textbf{(Ec. 60)}$$

Then:

$$FS = \frac{C/\gamma h + (1 - KSen\alpha / g)Cos\alpha Tan\phi}{Sen\alpha + KCos\alpha / g} \qquad \textbf{(Ec. 61)}$$

Where:

α = Angle of inclination of the fault plane
C = *Soil cohesion*
W = Weight of the sliding block
ϕ = Internal angle of friction of the soil
γ = Specific weight of the soil
K = Static friction factor
g = Gravitational acceleration

6.2.4.3 *Newmark's method*

Wieczorek *et al* (1985) developed criteria for evaluating the stability of slopes in a seismically-active region in its static state, and the seismic analysis of the slope fault developed by Newmark (1965). In general, in order to model the dynamic response of slopes, we can use the method of permanent displacement developed by Newmark (1965). This method was subsequently used to analyse the dynamic stability of natural hillsides (Jibson and Keefer, 1993) and to make at regional evaluations of the risk of landslide induced by earthquakes, using GIS (Jibson *et al*, 2000).

Newmark´s work consists of modelling a landslide as a rigid block and friction-causing block on an inclined plane (Figure 6-3). The block has a critical acceleration a_c, which represents the threshold acceleration required to overcome shear resistance and promote slippage.

Newmark´s analysis of landslides does not necessarily predict real landslides in the field, but it is a useful tool to define the comportment of any slope affected by the action of an earthquake.

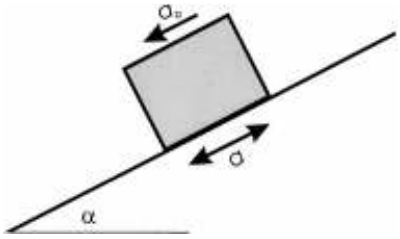

Figure 6-3
The inclined block scheme in Newmark´s analysis

Critical acceleration is a function of the static safety factor, and the geometry of the landslide. It can be expressed as follows:

$$a_c = (FS - 1) sen\alpha \qquad \textbf{(Ec. 62)}$$

Where a_c is critical acceleration (in terms of *t*, gravity acceleration), and FS is the safety factor in static conditions, and α is the angle of inclination of the terrain.

In this case, the angle α refers to the direction in which the centre of gravity of the mass movements when the landslide occurs. In an analysis on a regional scale, the value of the angle of thrust is practically equal to the angle of slope of the hillside.

The dynamic stability of the hillside, in the context of Newmark`s method, is related to static stability. For a regional analysis of landslides, the static method of the limit of equilibrium can be used, based on an infinite slope, considering a cohesive, friction-causing comportment for all slopes analysed. In fact, when the stability of hillsides is evaluated over large areas, it is not possible to use more exact methods, because the mechanical properties of materials and the geometry of the landslide are not known (Luzi *et al*, 2000).

Jaimes *et al* (2008) applied the Newmark method in the analysis of landslides by developing a simplified procedure which incorporates in an empirical equation to estimate Newmark´s landslide (D_N) as a functional intensity of the earthquake and critical acceleration (a_c). The expressions for cortical and subduction earthquakes respectively are:

$$\log D_N = -0.7819 + \log\left[\left(1 - \frac{a_c}{a_{\max}}\right)^{2.2627}\left(\frac{a_c}{a_{\max}}\right)^{-1.3779}\right] \pm 0.7351 \qquad \textbf{(Ec. 63)}$$

$$\log D_N = -1.2841 + \log\left[\left(1 - \frac{a_c}{a_{\max}}\right)^{1.9518}\left(\frac{a_c}{a_{\max}}\right)^{-1.2786}\right] \pm 0.5882 \qquad \textbf{(Ec. 64)}$$

Where *DN* is the displacement in centimetres, a_c is critical acceleration, and a_{max} is the maximum separation of ground (Jibson, 2007, Ambraseys and Menu, 1988).

Jibson (2007) and Ambraseys and Menu (1988) consider the value of displacement, D_N, of 5 cm as a critical value, which characterises the a fault in a slope, and promote a landslide. This conservative value represents slopes formed by fragile rock (Romeo, 2000). Jibson and Keefer (1993) define the value of D_N as 5-10 cm, being the critical value for faults in limo-arcillous slopes, and 10 cm for slopes formed by cohesive soils. In summary, values of D_N in the range of 5-10 cm increase the probability of a fault in the slope.

6.2.4.4 *Detailed method of rotational fault*

As a detailed method from the analysis of the likelihood of landslide, applicable in relatively small areas or regions, and with detailed information on conditions of susceptibility, we propose the use of a three-dimensional method of analysis, which takes account of possible rotational landslides in soil profiles characteristic of the zones with slopes and deposits which might become unstable. The analysis is made taking account of the digital elevation model of the terrain, the soil profile characteristic of the zones under study, the geotechnical properties characteristic of this defined soil profile, and the characterisation of detonating events, through the definition of an estimated depth of the water table, or of certain conditions of seismic hazard.

The method resolves the mechanical problem of slope stability using the using Bishop`s method of slices, with a three-dimensional expansion on a spherical surface. Based on these results, an assessment is made of the susceptibility to a landslide as a measurement of the hazard at each point in the defined analysis grid. The results are calibrated by the identification of critical points which present evidence of high susceptibility to slippage, either through complementary studies, or through past evidence of landslides. Figure 6-4 shows a representative scheme of the flow of data flows, and procedures in the model.

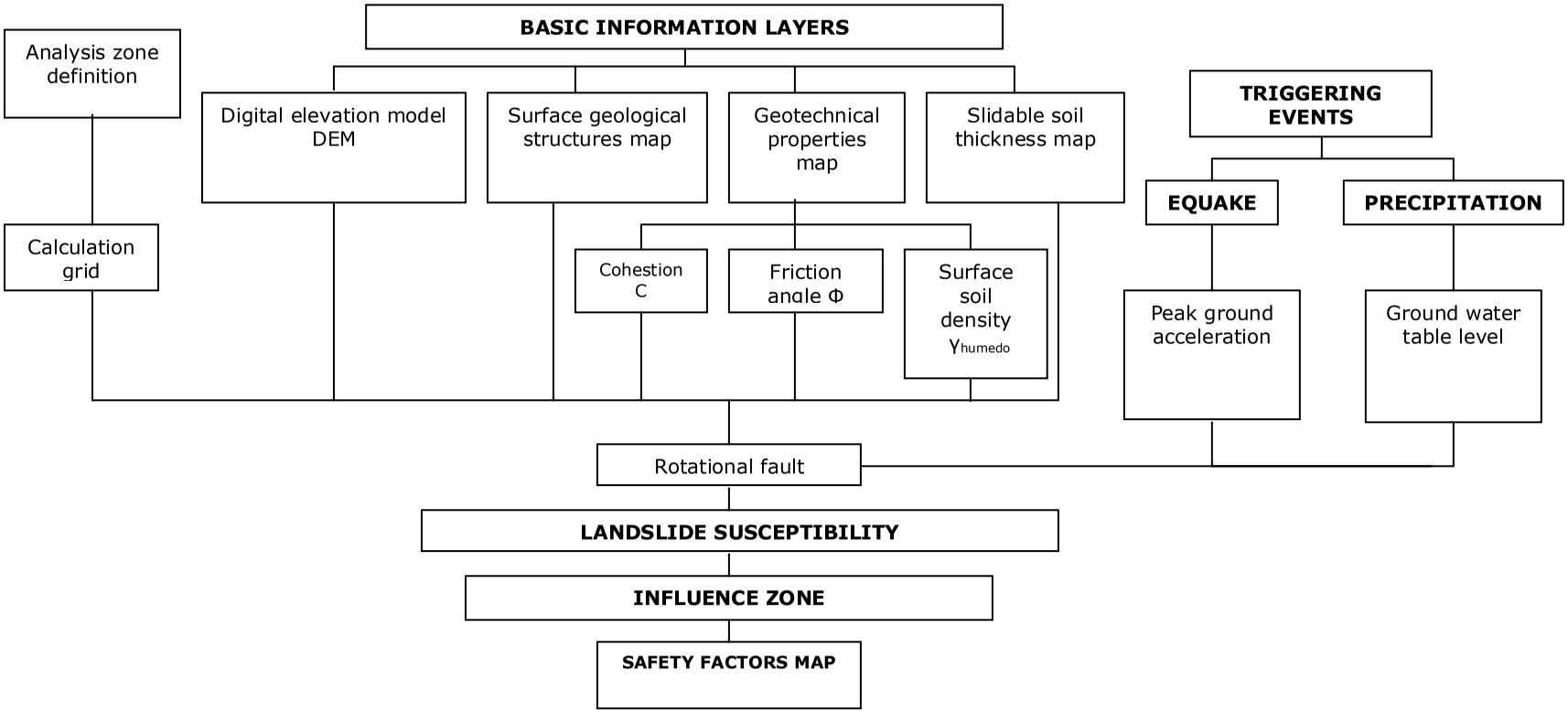

Figure 6-4
Method for the analysis of susceptibility to landslide

The calculation uses a three-dimensional slicing analysis of a sphere, whose geometrical variables are the radius and elevation at the centre. Other data are included, such as water tables, thickness, seismic hazard, and geotechnical parameters which affect stability.

The first step in the calculation consists of placing values for the radius and elevation at the centre, with respect to the surface of the ground. The information is manipulated by defining a square grid with a variable resolution, as shown in Figure 6-5.

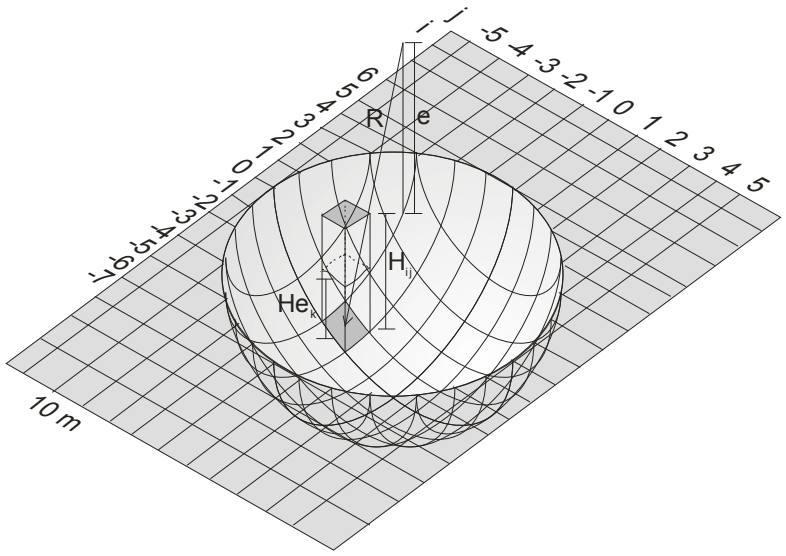

Figure 6-5
Three-dimensional surface of a spherical fault

The height for each slice is calculated:

$$H_{ij} = \sqrt{R^2 - l^2(i^2 + j^2)} + ct_{ij} - ct_{00} - e \qquad \textbf{(Ec. 65)}$$

Where:

H_{ij} = Height of the slice
R = Radius of the flat surface
l = Side of the cell
ij = Positioners
ct_{ij} = Elevation at the centre of the cell
ct_{00} = elevation at the central cell
e = Elevation of the centre of a sphere above ground

The resistant moment MR is calculated as follows:

$$\left|\vec{W}\right| = \sum_{k} \gamma_{ij}^{k}\left(S_r\right) H_{ij}^{k} \quad \textbf{(Ec. 66)}$$

$$r_N = (\sin\alpha_{ij}\cos\beta_{ij}, \sin\alpha_{ij} sen\beta_{ij}, \cos\alpha_{ij}) \quad \textbf{(Ec. 67)}$$

$$\vec{N} = \vec{W} \cdot \vec{r} \quad \textbf{(Ec. 68)}$$

$$MR = R\sum_{i,j}\left[\frac{c_{ij}(S_r)}{\cos\alpha_{ij}} + \left(\left|\vec{N}\right| - \frac{u_{ij}}{\cos\alpha_{ij}}\right)\tan\varphi_{ij}\right] \quad \textbf{(Ec. 69)}$$

Where:

W = Weight of the slice
γ_N = Vector in the direction of the radius
N = Normal force on the surface of the slice
c_{ij} = Apparent cohesion above saturation
S_r = Degree of soil saturation
γ_{ij}^{k} = Unit total weight of layer k, which is a function of the degree of saturation
H^{k}_{ij} = Height of stratum k
α_{ij} = Angle between vertical and the radius at the centre of the slice
β_{ij} = Angle between the projection of the radius on the horizontal plane and x-axis
ϕ_{ij} = Angle of friction for the layer
u_{ij} = Pressure of pores on fault surface

The total resistant moment is calculated as the sum of resistant moment at each site. The resistant moment is independent of the direction of slippage.

The actuating moment MA should be calculated considering that it is a three-dimensional problem, and this depends on the direction of slippage. Therefore, the concept of the critical direction of slippage is used, defined as the direction produced by the maximum actuating moment, and is associated with the direction of the highest slope, which means that it is directly dependent on topography. The actuating moment can be calculated using Equations 68-72

$$\vec{r}_T = (Cos\alpha_{ij} Cos\beta_{ij}, Cos\alpha_{ij} Sen\beta_{ij}, Sen\alpha_{ij}) \quad \textbf{(Ec. 70)}$$

$$\vec{T} = \vec{W} \cdot \vec{r}_T \quad \textbf{(Ec. 71)}$$

$$\vec{r}_D = (Cos\alpha_{ij} Cos\beta_{ij}^{d}, Cos\alpha_{ij} Sen\beta_{ij}^{d}, Sen\alpha_{ij}) \quad \textbf{(Ec. 72)}$$

$$\vec{\vec{T}}_d = \vec{\vec{T}} \cdot \vec{r}_D \quad \textbf{(Ec. 73)}$$

$$MA = R\sum_{ij}\left|T_d\right| \qquad \textbf{(Ec. 74)}$$

Where

r_T = Normal vector to the radius in the plane formed by the vertical and the radius
r_D = Normal vector to the radius in the slippage plane
T = Tangential force on the surface of the slice
T_d = Tangential force on the surface of the slice in the plane of the slice (Figure 6-6)

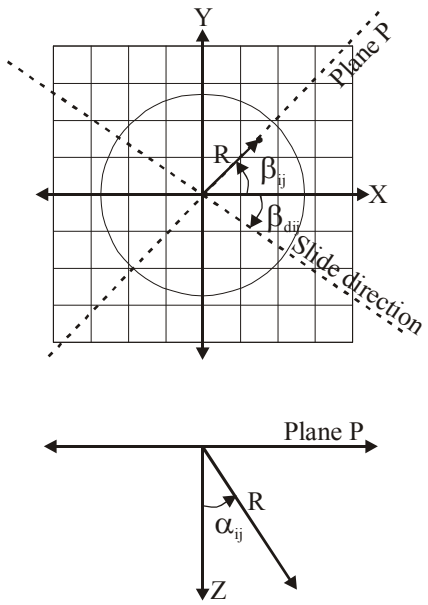

Figure 6-6.
Angles between planes

Finally, the safety factor is calculated as:

$$FS = \frac{MR}{MA} \qquad \textbf{(Ec. 75)}$$

The critical safety factor for the rotational fault hypothesis is obtained as the minimum value obtained after performing a number of iterations, changing the following variables: predominant direction of slippage, elevation of the centre of the sphere for calculation, and the radius of the sphere calculated. These parameters have several ranges specified by the user. Finally, the unsafety factor, FI, is calculated as the inverse of FS.

$$FI = \frac{1}{FS} \qquad \textbf{(Ec. 76)}$$

7 Evaluation model for volcanic hazard

7.1 Introduction

Volcanoes provide the only process which communicate the surface of the Earth with deep levels of the Earth's cortex. That is to say, they are the only means to observe and study lithological materials of magmatic origin, which form some 80% of the solid cortex. At the depths of the Earth's mantle, the magma under pressure rises, creating magmatic chambers within or below the cortex. The cracks in the cortex rock provide an outlet for the intense pressure, and this causes an eruption, with a range of materials such as water vapour, smoke, gases, ash, rock and lava, which are launched into the atmosphere in the process.

7.2 Principal volcanic products

A number of processes of eruption are generated in the context of volcanic activity, and they have an impact on nearby regions. The main processes are falling cold ash (ash/tephra), pyroclastic flows, lava flows, flows of cold rubble, and ballistic projections.

7.2.1 *Falling ash*

This process develops with the expulsion of fragments of magmatic material into the atmosphere (known as tephras or pyroclasts), driven by the rising gases produced during some volcanic eruptions. This mass of material is carried for great distances, depending on the prevailing wind, and scattered by atmospheric turbulence over wide areas, generating climatic change in zones far from the eruption itself. With the cooling and condensation of the mass of material, the material is deposited through the action of gravity on wide expanses of ground, causing damage not only in terms of climate but also in terms of property and infrastructure exposed to it.

Tephra is fragmented volcanic material, and classified by size, as shown in Table 7-1.

Table 7-1
Classification of tephra by size

Size (mm)	Clasification
> 64	***Bombs***
64 – 2	***Laphilli***
< 2	***Ash***

7.2.2 *Pyroclastic flows*

Pyroclastic flows are composed of granular material and eruption gases at high temperature, accumulated during the process of eruption in the eruption column, and whose high-intensity causes them to collapse, moving down the hillside with the product of the volcanic edifice, achieving high rates of flow; this is therefore one of the most destructive

processes of eruption which can occur. Their course is usually guided by the terrain, and can reach speeds of up to 200 m/sec, and temperatures of hundreds of degrees centigrade, detonating a number of combustible materials in their path.

7.2.3 *Lava flows*

Lava flows are currents of molten rock, which depending on chemical composition and dissolved gases, may vary in viscosity, and consequently in velocity and distance covered by the flow. The principal factors affecting the speed of a lava flow and the distances they cover depends principally on the characteristics of the matter expelled, although there are also factors such as the rate of expulsion, slope and accidents in the ground over which the lover spills, and the form or structure of the volcanic edifice. Like pyroclastic flows, lava flows generate almost total destruction along their path, because the very high temperatures scorch any element which in their path, even destroying the ground, which may take a long time to recover.

7.3 Volcanic Expolsivity Index

In 1982, vulcanologists Newhall C. of the US Geological Survey and S. Self of the University of Hawaii brought together quantitative measurements (volume of mass expelled, height of the smoke column) and qualitative information to propose an indicator for a volcanic explosivity index (VEI). The index is composed of eight classes, in which the index increases with the magnitude of the eruption and the volume of rock fragments expelled during it. Like the Richter scale, which measures seismic magnitudes, the volcanic explosivity index allocates a value to each level or order to reach level an order of magnitude as a factor of 10, for the volume of mass expelled. Table 7-2 describes each of the levels of the index proposed, and cites an example for each.

Table 7-2
Description of the volcanic explosivity index scale VEI
(source: http://www.ngdc.noaa.gov)

VEI	Eruptive column height (km)	Volume (m^3)	Description	Eruption type	Recurrence	Example
0	<0.1	$1x10^4$	Suave	Hawaian	Diaria	Kilauea
1	0.1-1	$1x10^6$	Efusiva	Haw/Strombolian	Diaria	Stromboli
2	1-5	$1x10^7$	Explosiva	Strom/Vulcanian	Semanal	Galeras, 1992
3	3-15	$1x10^8$	Explosiva	Vulcanian	Anual	Ruiz, 1985
4	10-25	$1x10^9$	Explosiva	Vulc/Plinian	Decenios	Galunggung, 1982
5	>25	$1x10^{10}$	Cataclísmica	Plinian	Siglos	St. Helens, 1981
6	>25 km	$1x10^{11}$	Paroxismal	Plin/Ultra-Plinian	Siglos	Krakatau, 1883
7	>25 km	$1x10^{12}$	Colosal	Ultra-Plinian	1.000 años	Tambora, 1815
8	>25 km	$>1x10^{12}$	Colosal	Ultra-Plinian	10.000 años	Toba (73,000 AC)

The Global Vulcanism Program of the Smithsonian IInstitution in the United States presents statistics of eruptions which have occurred in the last 10,000 years up to 1994, classified by the VEI. Figure 7-1 presents the distribution of this group of eruptions, classified on the VEI. It should be noted that no events have been recorded as higher than VEI range 8 during this period of observation.

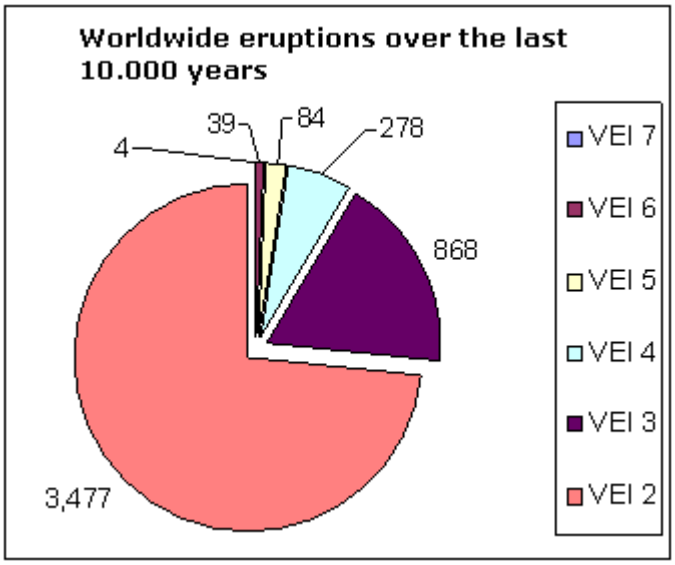

Figure 7-1
Statistics of eruptions occurring in the last 10,000 years
(Source: Global Vulcanism Program, Smithsonian Institution)

7.4 Evaluation models for falling ash

The first developments of models for the transport and deposition of particles as a consequence of volcanic eruptions were based on the input of the height of the eruption

column, wind velocity measured during some eruptions, and parameters determined on the basis of deposits from past eruptions. These models made quite rough assumptions, such as supposing a constant wind velocity, and particles which fall in accordance with their limit velocity. Most of the parameters used to characterise the model are calculated on the basis of empirical results compiled from previous eruptions.

7.4.1 *Advection-diffusion model*

Later, an advection-diffusion method was proposed, in which particles are dispersed by atmospheric turbulence, and the horizontal advection of wind, and are then deposited by the action of gravity. Suzuki (1983) proposed a two-dimensional model, consideringwind velocity, diffusivity, and the concentration of particles on a constant basis, with the timing of the falling of particles as a function of the limit velocity of falling. Additionally, the limit speed of falling incorporates parameters of shape and dimensions of particles, together with viscosity and density of the air.

7.4.2 *Models of distribution of matter in the smoke column*

Wood and Bursik (1991) present a model of distribution of particle sizes in accordance with a number of studies made in deposits of many past eruptions. This work provides a distribution of sizes, taking as normal distribution a parameter φ, defined as d=2- φ, where *d* is the diameter of the particle. Thus, the total volume of that size of particle is defined through a normal distribution.

In order to quantify the vertical distribution of matter expelled in the column, Suzuki (1983) requires a probability equation for the diffusion of particles varying with altitude in his theoretical model for the dispersion of ash.

$$P(z) = \frac{\beta^2 W_o \left[W_o \left(1 - \frac{z}{H_T} \right) - V_{\phi o} \right] \exp\left[-\beta \left(\frac{W_o}{V_{\phi o}} \left(1 - \frac{z}{H_T} \right) - 1 \right) \right]}{{V_{\phi o}}^2 H_T \left[1 - (1 + A) \exp(-A) \right]} \qquad \textbf{(Ec. 77)}$$

where H_t is the maximum height of the smoke column, A is a parameter which locates the point of maximum concentration of particles at a defined altitude as $Ht(1\text{-}1/A\phi)$, , and is calculated as $A\phi = A / V_{\phi o}$, , where A is the factor of the shape of the column, and $V_{\phi o}$ is the final velocity of the falling particles of size ϕ at sea level.

Armienti (1988) redimensions the problem of vertical distribution of matter, adopted by Suzuki (1983), and assumes the velocity of gas leaving the mouth of the eruption as a higher value of several orders in respect of the limit velocityof the falling particles.

7.4.3 *Dynamics of the smoke column*

Wood and Bursik (1991) and Bursikc (2001) present a model for predicting the dynamics of the smoke column, based on the convective model whose equations are derived from the

conservation of mass, conservation of moment, and conservation of energy, respectively, assimilating the column to a cylinder of average radius.

$$\frac{d}{dz}\left(\pi r^2 \rho u\right) = 2\pi r \rho_a u_e + \sum_{\varphi=1}^{N_\varphi} \frac{dM_\varphi}{dz} \qquad \textbf{(Ec. 78)}$$

$$\frac{d}{dz}\left(\pi r^2 \rho u^2\right) = \pi r^2 (\rho_a - \rho) g + u \sum_{\varphi=1}^{N_\varphi} \frac{dM_\varphi}{dz} \qquad \textbf{(Ec. 79)}$$

$$\frac{d}{dz}\left(\pi r^2 \rho u\left(c_v T + gz + \frac{1}{2}u^2 \right)\right) = 2\pi r \rho_a u_e \left(c_a T_a + gz + \frac{1}{2}u_e^{\,2} \right) + \left(c_p T + gz + \frac{1}{2}u^2 \right) \sum_{\varphi=1}^{N_\varphi} \frac{dM_\varphi}{dz} \qquad \textbf{(Ec. 80)}$$

Where the radius of smoke column is given by r, ρ is density of mass composed of air, particles and gases, u is the velocity of gases entering the system, T is temperature, and c_a and c_p are the specific heats of gases and the pyroclasts

7.4.4 *Models for the limit velocity of particles*

Wilson and Huang (1979) base the following expression on a number of tests of falling particles:

$$V_{\lim} = \frac{\rho_p g d^2}{9\mu_a F^{-0.64} + \sqrt{81\mu_a{}^2 F^{-0.64} + {}^3\!/_2\, \rho_a \rho_p g d^3 \sqrt{1.07 - F}}} \qquad \textbf{(Ec. 81)}$$

where d, F are the characteristic dimensions and coefficient of shape of the particles respectively, μ_a and ρ_p will be viscosity and density of the air respectively, and g is the value of gravity. This same result was to be used by Suzuki, to determine the time taken by particles in falling, in his model of advection-diffusion.

Bonadonna *et al* (1998) start with the model proposed by Sparks (1992) and Bursik (1992) and present a correction in the calculation of limit velocities for falling particles, according to the Reynolds number for each particle size; and they propose three equations:

$$\begin{aligned} V_{\lim} &\approx \sqrt{3.1 g \rho_p \, {}^d\!/_{\rho_a}} && \text{Re} > 500 \\ V_{\lim} &\approx d\left(4 g^2 \rho_p{}^2 / 255 \rho_a \mu_a\right)^{2/3} && 0.4 < \text{Re} < 500 \\ V_{\lim} &\approx g \rho_p d^2 / 18 \mu_a && \text{Re} < 0.4 \end{aligned} \qquad \textbf{(Ec. 82)}$$

7.4.5 *Programmes based on the advection-diffusion model*

Eurelian-type models propose the solution to the equation of particle diffusion by estimating the accumulation of particles on the ground, through the solution of equations for transport and sedimentation. In general, they are used for the prevention of emergencies, and for preparing plans for reducing disasters. These models include the

following, reported in literature:

ASHFALL Developed by Hurst and Turner (1999). In principle, this is was used as a system for civil prevention measures in the face of hazards from falling ash, and was later applied to the study of ash deposits during past eruptions

HAZMAP Developed by Macedonio (2005). This makes two strong approximations, namely the supposition of a horizontal and constant wind field, and the discarding of the vertical effect of advection-diffusion.

FALL3D Developed by Costa *et al* (2006). This includes complex processes such as wind fields and the diffusion tensor, and variation of conditions over short periods.

TEPHRA Developed by Connor *et al* (2001). This is based on density and the distribution of size in diffused particles in the smoke column, and the velocity of falling ash is a function of the variation in the Reynolds number.

7.5 Evaluation models for pyroclastic flows

Commonly, the hazard from pyroclastic flows is evaluated in specific terms for each case of analysis, and the study mainly refers to evidence of past eruptions and data recorded in some volcanoes around the world for which this kind of information is available. Some general models have been developed to evaluate the hazard, and they can be used in a fairly general manner, since they are based on the studies of comportment proper to flows, regardless of the characteristics of the volcano.

7.5.1 *Extension of flows*

Sheridan and Malin (1983) proposed a method for the evaluation of the area of influence of pyroclastic flows due to volcanic eruption. The method holds that the energy in the gas and particle cloud, which collapses from the column created by the eruption, diminishes with distance from the point of ejection, with the difference between the line of energy and topography. The line of energy is defined by the height of the eruption column and its angle of inclination. The angle is estimated based on statistical studies made of pyroclastic flows studied in eruptions observed. Figure 7-2 shows a scheme of the main considerations of the model (taken from Alberico *et al*, 2002).

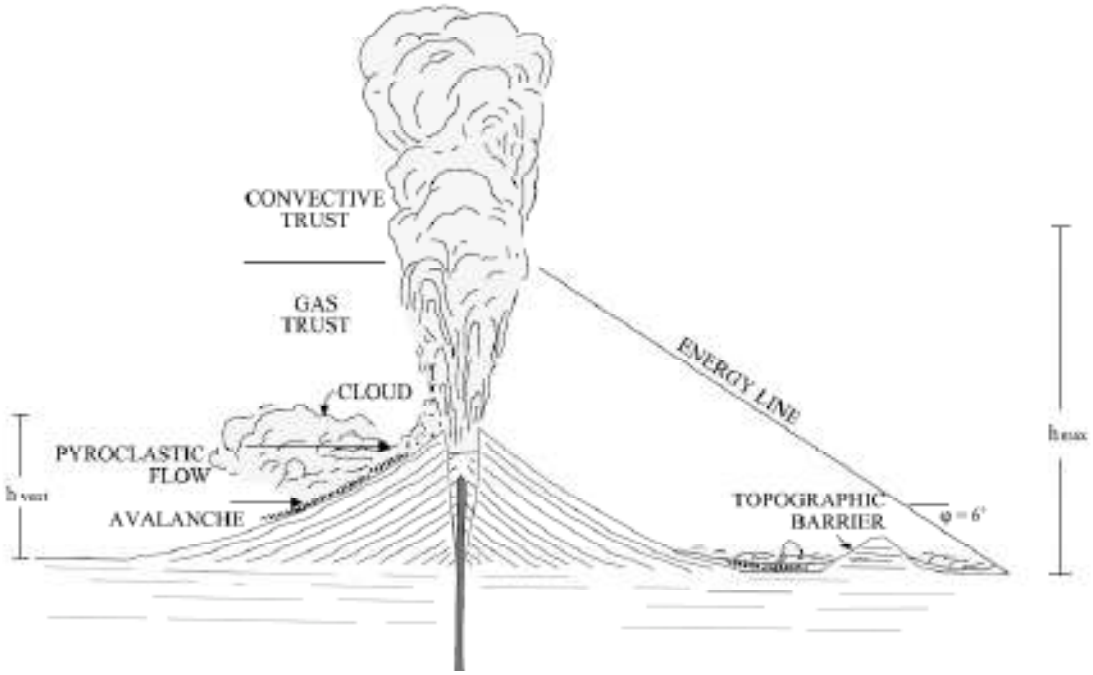

Figure 7-2
Estimate of the area of influence of pyroclastic flows, following Sheridan and Malin, 1982
(Source: Alberico et al., A methodology for the evaluation of long-term volcanic risk from pyroclastic flows in Campi Flegrei (Italy), Journal of Volcanology and Geothermal Research, N° 116, pp 63-78, 2002)

7.5.2 *Velocity of advance*

Pyroclastic flows are one of the most dangerous events which may occur as a consequence of volcanic eruption, and to a great extent this is due to the velocity of their advance. Typically, a pyroclastic flow may descend the slopes of the volcanic edifice at speeds of about 100 m/sec.

The velocity may be estimated based on the comportment of flow dynamics, through the relationship between inertial and kinetic force of the movement, given by the Froude number Fr, evaluated at the head of the current:

$$Fr = \frac{v_f}{\sqrt{g'h}} \qquad \textbf{(Ec. 83)}$$

where v_f corresponds to the speed of the flow, ages the height of the flow and $g.'$ is the reduced gravity calculated as:

$$g' = g\frac{\rho_c - \rho_a}{\rho_a} \qquad \textbf{(Ec. 84)}$$

Where ρ_c is the average density of the flow, ρ_a is the density of the air, and *g*. is gravity acceleration.

Nield and Woods (2004) obtained an empirical regression to approximate the Froude number, based on data compiled by Gröbelbauer in 1993. Their expression was the following:

$$Fr = 1.2\sqrt{2}\rho^* + 2.2\left(\frac{\rho^*}{2-\rho^*}\right)^{6.6} \quad \textbf{(Ec. 85)}$$

Where

$$\rho^* = \sqrt{\frac{|\rho_c - \rho_a|}{\rho_c + \rho_a}} \quad \textbf{(Ec. 86)}$$

7.5.3 *Temperature*

Flow temperature is the factor which has the greatest incidence on the loss of human life. Pyroclastic flows are typically expelled and temperatures of around 1000K. (Nield and Woods, 2004). As the flow advances, the turbulent comportment implies a mixture of the surrounding air into the flow, and this has incidence on the temperature of the total mass T_c, as a function of the relation of masses in the mixture (Nield and Woods, 2004), and the change in calorific energy of the mix for each degree of temperature:

$$T_c = \frac{m_{er}T_{er}\left[n_{er}C_v + (1-n_{er})C_s\right] + m_a C_a T_a}{m_{er}\left[n_{er}C_v + (1-n_{er})C_s\right] + m_a C_a} \quad \textbf{(Ec. 87)}$$

where m_{er} and m_a are masses of flow and air respectively, C_v and C_s are the specific heat for the portions of vapour and solid matter in the flowmass, C_a is the specific heat of air, n_{er} is the proportion of content in the mass of water vapour and solid matter in the flow, and T_{er} and T_a are the temperatures of the flow and of the air respectively.

7.6 Models of the passage of lava flows

Lava flows may be evaluated deterministically or probabilistically. For deterministic calculations, the problem is approached by the solution of the laws of the transport of viscous material, in which there are a number of parameters such as velocity, temperature, heat transfer and frontier conditions. This type of solution is highly complex, since the characteristic comportment of lava corresponds to non-Newtonian fluids.

Further, probabilistic models are fundamentally based on the topography of the site, determining the zones which are most likely to be invaded by the flow, even though other parameters may form part of the analysis.

7.6.1 *Model for determining lava flow tracks*

A series of empirical models have been proposed for probabilistic modelling, to establish the preferred route for a lava flow, basically founded on information compiled in the field from past eruptions

The model of the maximum probable slope, initially developed by Macedonio (1996) makes iterative calculations based on the Digital Elevation Model, to establish the probability that a cell will be invaded by lava, as the relationship between differences in altitude of the specific cell and its eight contiguous cells. The altitude of the cell analysed is corrected by a value for thickness, to take account of the depth or thickness of the flow.

Subsequently, Damián (2005) proposes an extended model, in which the value for the altitude of flow is not a constant as presented by the Felpeto (2001) calculating variations in it in accordance with a function F, as he does for the Digital Elevation Model, when increasing the height of the cell currently invaded, and the depth of the flow with it.

7.7 Analytical model proposed

7.7.1 *General*

The evaluation of volcanic hazards has become a constant discipline for a geological agents and institutions in countries where there is constant volcanic activity. Most of the other variations of the hazard are made by vulcanologists at the request of disaster management agencies, and most are used to prepare emergency plans associated with each particular active volcano.

The inclusion of quantitative considerations in the evaluation of volcanic hazards began only about 10 years ago, and complete probabilistic analyses of volcanic hazards only exists for a few volcanoes (Young *et al* 1998, Young and Sparks, 1998).

Comprehensive studies of volcanic hazards are relatively scanty, mainly due to the lack of reliable information. In addition, most of the analysis of volcanic hazards have been conducted with an emphasis on the effects on the population, and not the evaluation of economic impact, that is, the evaluation of loss of life and not of economic loss (Young and Sparks, 1898, Young *et al*, 1998).

7.7.2 *Selection*

Distribution models were selected for volcanic products due to the hazard of lava flows, pyroclastic flows and falling ash, in a probabilistic context which allowed the identification of the frequency of recurrence of eruptions of a given magnitude. The distribution models were defined in order to characterise the hazard, through intensities which could be related to damage, and the comportment of infrastructure exposed to them, such that they would be and applicable to subsequent risk analysis.

7.7.3 *Procedure for analysis*

Figure 7-3 presents the flow diagram of the volcanic hazard model, which is based on the definition of particular scenarios, allocating a specific frequency of occurrence to each type of scenario. Intensities associated with them are determined by distribution evaluation models for volcanic products.

(1) *Definition and general characterisation of active volcanoes*. Based on available information (geology, geomorphology, hazard studies), the characteristics of active volcanoes are defined, including type, type of product, and explosivity index (VEI) at the maximum recorded. Volcanoes are considered to be active if they have proven activity in the last 10,000 years.

(2) *Definition of recurrence of events based on historical information*. Based on the catalogue of historical eruptions, rates of excedence are determined for specific values of VEI.

(3) *Characterisation of intensity of eruptions, as a function of VEI.* Based on information compiled on historical eruptions in the volcano, the intensity of an eruption of a particular volcano is defined as a function of VEI. This definition of intensity is particular to each volcano, and should be defined by the products which the volcano may generate.

(4) *Geographical location of possible centres of volcanic emission*. Based on the morphology of a volcanic edifice, specific sites or defined centres of emission, a definition is made of sites where matter may begin to be expelled. If the information allows, it will also be possible to define a function of probability of the emission from different sites identified.

(5) *Distribution modelling of volcanic products*. An evaluation is made of each scenario based on magnitude in terms of VEI, and intensity in terms of the parameters proper to each distribution model. The calculation of distribution generates zones of affectation and specific local intensity for the magnitude selected. Three types of products are considered: falling ash, lava flows and pyroclastic flows.

(6) *Generation of hazard maps for representative events*. Spatial distribution maps will be generated for products and associated intensities for each defined event, through the distribution models adopted.

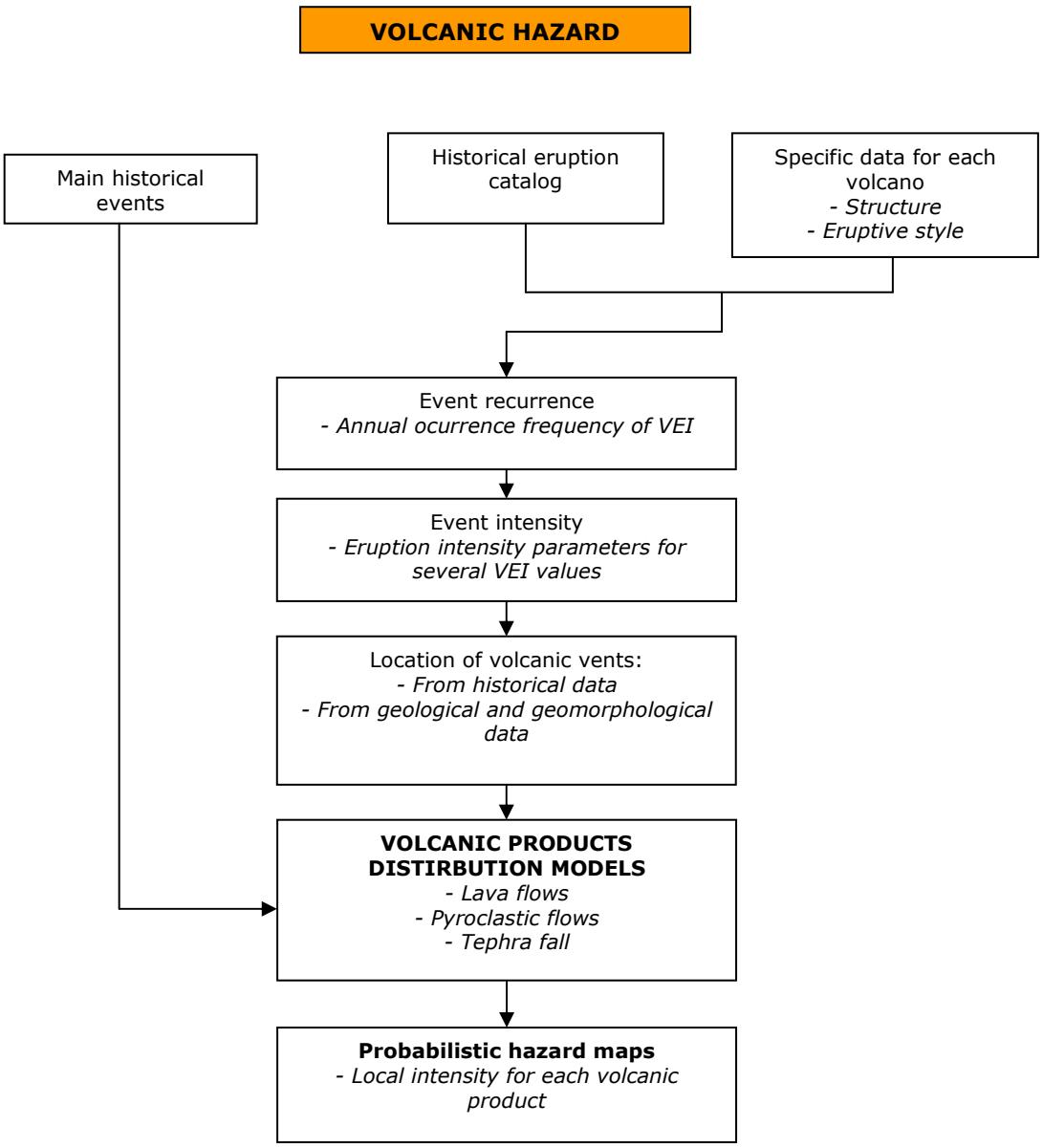

Figure 7-3
Flow diagram of the module for volcanic hazard

7.7.4 *Distribution model for falling ash*

The distribution model for volcanic ash employed is an advection-diffusion model, in which particles are diffused by atmospheric turbulence, and horizontal advection of the wind, and are then deposited by the action of gravity (Folch and Felpeto, 2005). The general equation which is the basis of the model is (Armienti *et al*, 1988):

$$\frac{\partial C}{\partial t}+V_x\frac{\partial C}{\partial x}+V_y\frac{\partial C}{\partial y}+V_z\frac{\partial C}{\partial z}-\frac{\partial vC}{\partial z}=\frac{\partial}{\partial x}\left(k_x\frac{\partial C}{\partial x}\right)+\frac{\partial}{\partial y}\left(k_y\frac{\partial C}{\partial t}\right)+\frac{\partial}{\partial z}\left(k_z\frac{\partial C}{\partial z}\right)+S \qquad \textbf{(Ec. 88)}$$

Where, C is the concentration of particles, k_x. k_y and k_z, are the components of the diffusivity tensor, Vx, Vy and Vz define the velocities field of the system, v is the limit velocity for falling particles, and S is the function which describes the entry of the particles into this column. For ease of solution of the problem, we consider that the wind currents and vertical diffusion may be ignored, and that the coefficients of horizontal diffusion equal ($k=k_x=k_y$).

The granulometric distribution is defined as a function of the parameter φ, defined as $d=2^{-\varphi}$, and d is the particle diameter. Therefore, the total volume of that size particle is defined as (Wood and Bursik, 1991)

$$V_\varphi=\frac{V}{\sqrt{2\pi\sigma_\varphi}}\exp\left(\frac{(\varphi-\varphi_m)^2}{2\sigma_\varphi{}^2}\right) \qquad \textbf{(Ec. 89)}$$

Where V is the total volume emitted, φ_m and σ_φ are the median and standard deviation of distribution of the parameter φ.

The distribution of matter expelled in the column is modelled by assuming an exit velocity for the gas in the mouth of the eruption as a value of several orders of magnitude higher than the limit velocity of falling particles (Armienti *et al*, 1988)

$$V_\phi(z)=V_\phi\frac{A_\phi{}^2\left(1-\frac{z}{H_T}\right)\exp\left(A_\phi\left(\frac{z}{H_T}-1\right)\right)}{H_T\left(1-\left(1+A_\phi\right)\exp\left(-A_\phi\right)\right)} \qquad \textbf{(Ec. 90)}$$

where H_T is the maximum height of the smoke column, and A_φ is a parameter for the location of the point of maximum concentration of particles at a given altitude, defined as $H_T(1-1/A_\phi)$, , and is calculated as a $A_\phi = A/v_{\phi 0}$,, where A is a factor of the shape of the column and $v_{\phi 0}$ is the final speed of falling particles of size φ at sea level.

The eruptive column is divided into N layers of the same height Δz, in which it is assumed that the windfield and terminal velocity of particles remain constant, such that the concentration of mass with a volume $V_{\phi j}$, located at altitude z_j will be transferred by the effect of wind currents and free falling of particles of size φ to a point located at coordinates $x_{\phi j}$, and $y_{\phi j}$, given by (Folch y Felpeto, 2005).

$$x_{\phi j} = x_o + \sum_{i=j}^{1} W_{xi} \frac{z_i - z_{i-1}}{v_{\phi i}}$$
$$y_{\phi j} = y_o + \sum_{i=j}^{1} W_{yi} \frac{z_i - z_{i-1}}{v_{\phi i}} \qquad \textbf{(Ec. 91)}$$

Where x_o and y_o are the coordinates of the centre of emission. It is also assumed that the entire mass is emitted at the same instant $t=0$. The total time necessary for a mass of particles to cross all the layers from a position z_j is:

$$t_{fall} = \sum_{i=1}^{j} \Delta t_i \qquad \textbf{(Ec. 92)}$$

Hence, the thickness deposited by particles of size φ. with initial circular distribution in a radius r_0, initially located at a altitude z_j is (Carslaw and Jaeger, 1959):

$$T_{\phi j} = \frac{V_{\phi j}}{2\pi r_0^2}\left[erf\left(\frac{r_0 + r}{2\sqrt{kt_{fall}}}\right) + erf\left(\frac{r_0 - r}{2\sqrt{kt_{fall}}}\right)\right] erf\left(\frac{r_0}{2\sqrt{kt_{fall}}}\right) \qquad \textbf{(Ec. 93)}$$

Where r is the distance between the centre of initial concentration ($x_{0\phi j}$, $y_{0\phi j}$), and the point where the thickness is being evaluated, and *erf* corresponds to the Gaussian error function. Finally, the total thickness of particles deposited is calculated as the sum of the contributions of all the layers of the column and all sizes of particle considered.

$$T = \sum_{\phi \min}^{\phi \max} \sum_{j=1}^{N} T_{\phi j} \qquad \textbf{(Ec. 94)}$$

The terminal velocity is particles is calculated as a function of the Reynolds number, as follows (Banadonna *et al*, 1998)

$$V = \sqrt{\frac{8\rho_p d g}{6\rho_a D}} \qquad \text{Re} > 500$$
$$V = d\left(\frac{4g^2 {\rho_p}^2}{255\rho_a \mu_a}\right)^{2/3} \qquad 0.4 < \text{Re} < 500 \qquad \textbf{(Ec. 95)}$$
$$V = \frac{g\rho_p d^2}{18\mu_a} \qquad \text{Re} < 0.4$$

Where ρ_p is the density of particles, d is the particle diameter, ρ_a is the density of air, D is the drag parameter, and μa is the viscosity of air:

7.7.5 *Model of distribution for lava flows*

A runoff model for basins is used to model the spread of lava flows, and this is indicative of all possible routes which a given flow might take when emitted from a particular point, as a function of the particular topography of the volcano. The model verifies the difference in altitude between contiguous cells on the Digital Elevation Model, to determine where the lava flow may run off. This operation is repeated until a maximum value is obtained for the distance from the centre of emission, which is given as a function of the particular VEI of the eruption, and the characteristics of the volcano itself.

7.7.6 *Distribution model for pyroclastic flows*

The Energy Cone model is used (Sheridan and Malin, 1992) to characterise the probable spread of pyroclastic flows in a given eruption. In this model, the energy of the gas and particle cloud, which collapses from the columns created by the eruption, diminishes with distance from the point of ejection, with the difference between the line of energy and topography. The liability as defined by the height of the column of eruption, and the estimated angle of inclination of the cone, which relates a height of the height of the column with the probable spread of impact of the flow (Figure 7-2).

The susceptibility of a given site is defined as a function of the magnitude of available energy which the flow has at that point. The magnitude of energy age is defined as:

$$h = H_0 + H_c - d\tan(\alpha_c) - h_0 \qquad \textbf{(Ec. 96)}$$

Where H_0 is the topographical altitude of the centre of emission, H_c is the estimated altitude of the column, d is the distance between the centre of emission and the point analysed, αc is the angle of the cone, and h_0 is the topographic altitude of the point analysed.

8 References

Alberico, I., Lirer, L.,Petrosino, P., Scandone, R., 2002. A methodology for the evaluation of long-term volcanic risk from pyroclastic flows in Campi Flegre (Italy). J. Vol. Geoth. Res. 166, 63-78.

Alcántara-Ayala, I. (2004). Hazard assessment of rainfall-induces landsliding in Mexico. Geomorphology, 61, 19-14.

Alexander, D., (1989), Urban landslides, Progress in Physical Geography, Vol. 13, pp. 157 - 191.Ambraseys, N.N., Menu, J.M., (1988), Earthquake-induced ground displacements, Earthquake Engineering and Structural Dynamics, Vol. 16, pp. 985–1006.

Araña, V. Felpeto, A. M. Astiz, A. García, R. Ortiz and R. Abella, 2000.Zonation of the main volcanic hazards (lava flows and ash fall) in Tenerife, Canary Islands. A proposal for a surveillance network, Journal of Volcanology and Geothermal Research, Volume 103, Issues 1-4, Pages 377-391

Armienti, P., G. Macedonio y M. Pareschi (1988). A Numerical Model for Simulation of Tephra Transport and Deposition: Applications to May 18, 1980, Mount St. Helens Eruption, J. Geophys. Res., 93(B6), 6463-6476.

Avelar C, (2006) "Expresiones para modificar el intervalo de promediación en la velocidad de viento, entre los resultados de un modelo paramétrico y los boletines de huracanes". Reporte Interno, ERN Ingenieros Consultores, julio 2006.

Avelar C, (2006-2) "Procedimiento para determinar áreas de exposición ante los efectos del viento y asignar factores de topografía". Reporte Interno, ERN Ingenieros Consultores, julio 2006.

Barrantes, J., Vega, N., 2003. La persistencia y las cadenas de Markov aplicadas a la lluvia en San José durante el periodo 1950-1990. Topography Meteorology and Oceanography 10. 2003. Pag: 12-19.

Barrantes Castillo, G. 1996 Zonificación de amenazas por inundación en el valle del Río Sixaola. San José: Costa Rica. Universidad Nacional (UNA). Escuela de Ciencias Geográficas; 1996. Documento N°: 289.

Biswajeet Pradhan, Saro Lee. 2007. Utilization of Optical Remote Sensing Data and GIS Tools for Regional Landslide Hazard Analysis Using an Artificial Neural Network Model. Earth Science Frontiers. 2007. Pag: 143–152.

Bonadonna, C., Ernst, G., Sparks, R., 1998. Thickness variations and volume estimates of tephra fall deposits: the importance of the particle Raynolds number. J. Volcanol. Geotherm. Res. 81 (3-4), 173-187.

Boore, D.M., 1983. Stochastic simulation of high-frequency ground motion based on seismological models of radiated spectra, Bull. Seism. Soc. Am. 73, 1865-1884

Brune, J.N., 1970. Tectonic stress and the spectra of seismic S waves from earth, J. Geophy. Res. 75, 4997-5009.

Bursik, M. (2001). Effect of Wind on the Rise Height of Volcanic Plumes, Geophys. Res. Lett., 28(18), 3621-3624.

Bursik, M. R S J Sparks, J S Gilbert and S N Carey, 1992. Sedimentation of tephra by volcanic plumes: I. Theory and its comparison with a study of the Fogo A plinian deposit, Sao Miguel (Azores), Bulletin of Volcanology, Volume 54, Number 4, 329-344.

Caballero, L., Macías, J.L., García-Palomo, A., Saucedo, G.R., Borselli, L., Sarocchi, D., Sánchez, J.M. (2006). The September 8-9, 1998 rain-triggered flood events at Motozintla, Chiapas, Mexico. Natural Hazards, 39: 103-126.

Carrara, F. Guzzetti, M. Cardinali and P. Reichenbach. 1999. Use of GIS Technology in the Prediction and Monitoring of Landslide Hazard. Natural Hazards 20. 1999. Pag: 117–135.

Carslaw, H., Jaeger, J., 1959. Conduction of Heat in Solids. Clarendon Press, Oxford.

Cees J. Van Westen. 2000. The Modelling of Landslide Hazards Using Gis. Surveys in Geophysics 21. 2000. Pag: 241–255.

Chang-Jo Chung, Andrea G. Fabbri. 2008 Predicting landslides for risk analysis — Spatial models tested by a cross-validation technique. Elsevier. Geomorphology 94. 2008. Pag 438–452.

Chien-chih Chen, Chih-Yuan Tseng, Jia-Jyun Dong. 2007. New entropy-based method for variables selection and its application to the debris-flow hazard assessment. Elsevier. Engineering Geology 94. 2007. Pag 19–26.

Chow, V. T. (editor) 1964. Handbook of applied hydrology. Mc Graw-Hill. New York, 1964

Climent, A., Taylor, W., Ciudad Real, M., Strauch, W., Villagram, M., Dahle, A., Bungum, H., 1994. Spectral strong-motion attenuation in Central America, NORSAR Technical Report, No. 2-17, 46 pp.

Connor, C.B., B.E. Hill, B. Winfrey, N.M. Franklin, and P.C. La Femina, Estimation of volcanic hazards from tephra fallout, Natural Hazards Review, 2 (1), 33-42, 2001.

Costa, A., G. Macedonio and A. Folch, 2006. A three-dimensional Eulerian model for transport and deposition of volcanic ashes, Earth and Planetary Science Letters, 241 (3-4), 634-647

Douglas, J., Bungum, H., Dahle, A., Lindholm, C., Climent, A., Taylor, W., Santos, P., Schmidt, V., Strauch, W., 2004. Strong Motion Datascape Navigator.

Felpeto A, "User's Guide - VORIS - Volcanic Risk Information System- ", Observatorio Geofísico Central - IGN - , Septiembre 2007.

Felpeto, A. Joan Martí, Ramon Ortiz, 2007. Automatic GIS-based system for volcanic hazard assessment, Journal of Volcanology and Geothermal Research, Volume 166, Issue 2, 1 October 2007, Pages 106-116.

Felpeto, A. V. Araña, R. Ortiz, M. Astiz and A. García, 2001. Assessment and Modelling of Lava Flow Hazard on Lanzarote (Canary Islands), Natural Hazards, Volume 23, Numbers 2-3, 247-257.

Felpeto, A., Garcia, A., Ortiz, R., 1996. Mapas de riesgo. Modelizacion. In: Ortiz, R. (Eds.), Riesgo Volcanico, Serie Casa de los Volcanes, Servicio de Publicaciones del Cabildo de Lanzarote, Spain, vol. 5, pp. 67–98.

FEMA. Multi-hazard Loss Estimation Methodology. Flood Model. Department of Homeland Security Federal Emergency Management Agency. Mitigation Division. Washington, D.C.National Institute of Building Sciences. HAZUS-MH MR3 Technical Manual. Pag: 1-471

Florian Pappenberger, Keith J. Beven, Marco Ratto, Patrick Matgen. 2008. Multi-method global sensitivity analysis of flood inundation models. Advances in Water Resources 31. 2008. Pag: 1–14.

Folch, A., Felpeto, A., 2005. A coupled model for dispersal of tephra during sustained explosive eruptions. J. Volcanol. Geotherm. Res., 145. 337-349

G. Schumann, P. Matgen, L. Hoffmann, R. Hostache, F. Pappenberger, L. Pfister. 2007. Deriving distributed roughness values from satellite radar data for flood inundation modelling. Journal of Hydrology 344. 2007. Pag: 96– 111.

Gabet E.J. y Mudd S., (2006), The mobilization of debris flows from shallow landslides, Geomorphology, Vol. 74, pp. 207-218.

H. Chen, C.F. Lee. 2003. A dynamic model for rainfall-induced landslides on natural slopes. Elsevier. Geomorphology 51. 2003. Pag 269–288.

Hanks, T. C. y H. Kanamori, 1979. A moment magnitude scale, J. Geophys. Res., No. 84, Pag. 2348– 2350.

H.L. Perotto-Baldiviezo, T.L. Thurowb, C.T. Smith, R.F. Fisher, X.B. Wu. 2004. GIS-based spatial analysis and modeling for landslide hazard assessment in steeplands, southern Honduras. Elsevier. Agriculture, Ecosystems and Environment 103. 2004. Pag.165–176.

Helal, M.A., Mehanna, M.S., 2008. Tsunami form nature to physics, Chaos, Solitons and Fractals, 36, 787-796.

Hurst, A.W., and R. Turner, 1999. Performance of the program ASHFALL for forecasting ashfall during the 1995 and 1996 eruptions of Ruapehu volcano, New Zealand Journal of Geology and Geophysics, 42 (4), 615-622

Jaimes M.A., Niño M., Reinoso E., Avelar C. y Huerta B. (2008), Metodología para estimación de daño en la infraestructura por deslizamientos usando sistemas de información geográfica, XVI Congreso Nacional de Ingeniería Estructural, Veracruz, México.

Jeffrey C. Neal, Peter M. Atkinson, Craig W. Hutton. 2007. Flood inundation model updating using an ensemble Kalman filter and spatially distributed measurements. Journal of Hydrology 336. 2007. Pag: 401– 415.

Jibson R.W., Harp E. L. y Michael J.A. (2000), A method for producing digital probabilistic seismic landslide hazard maps, Engineering Geology, Vol. 58, pp. 271-289.

Jibson R.W. y Keefer D.K., (1993), Analysis of the seismic origin of landslides: examples from the NewMadrid seismic zone, Geological Society of America Bulletin, Vol. 105, pp. 521–536.

Jibson R. (2007), Regression models for estimating coseismic landslide displacement, Engineering Geology, Vol. 91, pp. 209-218.John F. England Jr, Mark L. Velleux, Pierre Y. Julien. 2007. Two-dimensional simulations of extreme floods on a large watershed. Journal of Hydrology 347. 2007. Pag: 229– 241.

K.M. Neaupane, M. Piantanakulchai. Analytic network process model for landslide hazard zonation. Elsevier. Engineering Geology 85. 2006. Pag. 281–294.

Katz, R. W., y Parlange M. B. 1995. Generalizations of Chain-Dependent Processes: Application to Hourly Precipitation, Water Resources Research, Vol. 31(5), 1331-1341.

Keefer D.K., (1984), Landslides caused by earthquake, Geological Society of America Bulletin Vol. 95, pp. 406–421.

Keefer D.K., (2002), Investigating landslides caused by earthquakes - A historical review, Survey in Geophysics, Vol. 23, pp. 473-510

Kramer S., Geotechnical Earthquake Engineering, Ed. Prentice Hall, 1996

Leonardo Ermini, Filippo Catani, Nicola Casagli. Artificial Neural Networks applied to landslide susceptibility assessment. Elsevier. Geomorphology 66. 2005. Pag. 327–343.

Luzi L., Pergalani F. y Terlien M.T.J. (2000), Slope vulnerability to earthquakes at subregional scale, using probabilistic techniques and geographic information systems, Engineering Geology, Vol. 58, pp. 313-336.

M.D. Ferentinou, M.G. Sakellariou. Computational intelligence tools for the prediction of slope performance. Elsevier. Computers and Geotechnics 34. 2007. Pag. 362–384.

M.H. Hsu, S.H. Chen, T.J. Chang, 2000. Inundation simulation for urban drainage basin with storm sewer system. Elsevier. Journal of Hydrology 234. 2000. Pag: 21–37.

Macedonio, G., 1996. Modelling lava flow hazard. In: Barberi, F., Casale, R. (Eds), The Mitigation of Volcanic Hazards, Office for Official Publications of the European Communities, Luxembourg, pp. 89–95.

Macedonio, G., A. Neri, J. Martì and A. Folch, 2005. Temporal evolution of flow conditions in sustained magmatic explosive eruptions, Journal of Volcanology and Geothermal Research, Volume 143, Issues 1-3, 1 May 2005, Pages 153-172.

Macedonio, G., M. Pareschi, and R. Santacroce (1988). A Numerical Simulation of the Plinian Fall Phase of 79 A.D. Eruption of Vesuvius, J. Geophys. Res., 93(B12), 14817-14827.

McGure, R.K., Hanks, T.C., 1981. The character of high frequency strong motion, Bull. Seism. Soc. Am. 71, 2071-2095.

Montero, W., Peraldo, G., Rojas, W., 1997. Proyecto de amenaza sísmica de América Central. Informe final del proyecto del Instituto Panamericano de Geografía e Historia (IPGH), Septiembre 1997: 79 p.

Mora, S., Vahrson, W.G., (1993), Determinación "a priori" de la amenaza de deslizamientos utilizando indicadores morfodinámicos, Tecnología ICE, Vol. 3, No. 1, pp. 32 - 42.

Mowen Xie, Tetsuro Esaki and Guoyun Zhou. GIS-Based Probabilistic Mapping of Landslide Hazard Using a Three-Dimensional Deterministic Model. Natural Hazards 33. 2004. Pag 265-282.

Mowen Xie, Tetsuro Esaki, Meifeng Cai. A time-space based approach for mapping rainfall-induced shallow landslide hazard. Environmental Geology. 2004. Pag. 840–850.

Mowen, Xie., Esaki, Tetsuro., Cheng, Qiu., Lin, Jia., 2007. Spatial three-dimensional landslide susceptibility mapping tool and its applications. Earth Science Frontiers. 2007. Pag: 73–84.

Mu Jin-Bin, Zhang Xiao-Feng. 2007. Real-Time Flood Forecasting Method With 1-D Unsteady Flow Model. Journal of Hydrodynamics 19(2). 2007. Pag: 150-154.

Newhall, C., y S. Self (1982). The Volcanic Explosivity Index (VEI) An Estimate of Explosive Magnitude for Historical Volcanism, J. Geophys. Res., 87(C2), 1231-1238.

Newmark N. (1965), Effects of earthquakes on dams and embankments, Geotechnique Vol. 15, pp.137-160.

Okal, E.A. y C.E. Synolakis, 2004, Source discriminants for near-field tsunamis, Geophys. J. Intl., No. 158, Pag. 899-912

Organización Meteorológica Mundial, OMM, 1969. Manual for Depth – Area – Duration Analysis for Strom Precipitation, WMO – No. 237, TP 129, Ginebra, Suiza, 1969.

Organización Meteorológica Mundial, OMM, 1981. Selection of Distribution Types for Extremes of Precipitation, WMO – No. 560, Ginebra, Suiza, 1981.

P. Matgen , G. Schumann , J.-B. Henry, L. Hoffmann, L. Pfister. 2007. Integration of SAR-derived river inundation areas, high-precision topographic data and a river flow

Paul D. Bates, Matthew D. Wilson, Matthew S. Horritt, David C. Mason, Nick Holden, Anthony Currie. 2006. Reach scale floodplain inundation dynamics observed using airborne synthetic aperture radar imagery: Data analysis and modelling. Journal of Hydrology 328. 2006. Pag: 306– 318.

Paul L. Wilkinson, Malcolm G. Anderson, David M. Lloyd, Jean-Philippe Renaud. Landslide hazard and bioengineering: towards providing improved decision support through integrated numerical model development. Elsevier. Environmental Modelling & Software 17. 2002. Pag. 333–344

R. Mehrotra, R. Srikanthan, Ashish Sharma. 2006. A comparison of three stochastic multi-site precipitation occurrence generators. Elsevier. Journal of Hydrology 331. 2006. Pag: 280-292.

Roberto A. T. Gomes, Renato F. Guimara, Osmar A. Carvalho Jr, Nelson F. Fernandes, Eurípedes A. Vargas Jr, Eder S. Martins. Identification of the affected areas by mass movement through a physically based model of landslide hazard combined with an empirical model of debris flow. Nat Hazards. 2008. Pag. 197–209.

Romeo, R., 2000. Seismically induced landslide displacements: a predictive model. Elsevier. Engineering Geology 58. 2000. Pag: 337–351.

Rojas W., 1993. Catálogo de Sismicidad Histórica y Reciente en América Central: Desarrollo y Análisis. Universidad de Costa Rica. Escuela Centroamericana de Geología.

Rojas W., Cowan H., Lindholm C., Dahle A., Bungum H., 1993. Regional Seismic Zonation for Central America: A Preliminary Model. Reduction of Natural Disasters in

Rutger Dankers , Ole Bøssing Christensen, Luc Feyen, Milan Kalas, Ad de Roo. 2007. Evaluation of very high-resolution climate model data for simulating flood hazards in the Upper Danube Basin. Journal of Hydrology 347. 2007. Pag: 319– 331.

S. Poli and S. Sterlacchini. Landslide Representation Strategies in Susceptibility Studies using Weights-of-Evidence Modeling Technique, Natural Resources Research, Vol. 16, No. 2, June 2007. Pag 121- 134.

Saro Lee, Moung-Jin Lee. Detecting landslide location using KOMPSAT 1 and its application to landslide-susceptibility mapping at the Gangneung area, Korea. Elsevier. Advances in Space Research 38. 2006. Pag 2261–2271.

Saro Lee. Application of Likelihood Ratio and Logistic Regression Models to landslide Susceptibility Mapping Using GIS. Environmental Management Vol. 34, No. 2. Springerlink. 2004. Pag. 223–232

Satake, K. 2002. Tsunamis, en Lee, W., Kanamori, H., Jennings, P., Kisslinger, C., (editores), International Handbook of Earthquake and Engineering Seismology, 81A, 437-451.

Schmidt V., Dahle A., Bungum H., 1997. Costa Rican Spectral Strong Motion Attenuation. Reduction of Natural Disasters in Central America. NORSAR.

Sedki, D. Ouazar E. El Mazoudi. 2008.Evolving neural network using real coded genetic algorithm for daily rainfall-runoff forecasting. Expert Systems with Applications. 2008. Pag: 1-11.

Sheridan,M.F.,Malin, M.C.,1983. Application of computer assisted mapping to volcanic hazard evaluation of surge eruptions: Vulcano,Lipari and Vesuvius. J. Volcanol. Geotherm. Res. 17,187-202.

Sparks, R.S.J., Bursik, M.I., Ablay, G.J., Thomas, R.M.E., Carey, S.N., 1992. Sedimentation of tephra by volcanic plumes: Part 2 - Controls on thickness and grain size variations on tephra fall deposits. Bull. Volcanol. 54, 685– 695.

Suzuki, T., 1983. A theoretical model for dispersion of tephra. En: Shimozuru, D., Yokoyama, I. (Eds.), Arc Volcanism, Physics and Tectonics. Terra Scientific Publishing Company, Tokyo.

T. Iida. A stochastic hydro-geomorphological model for shallow landsliding due to rainstorm. Elsevier. Catena 34. 1999. Pag. 293–313.

Taylor, W., Santos, P., Dahle, A., Bungum H., 1992. Digitization of Strong Motion Data and PGA Attenuation. NORSAR.

Thiery, J.-P. Malet, S. Sterlacchini, A. Puissant, O. Maquaire. Landslide susceptibility assessment by bivariate methods at large scales: Application to a complex mountainous environment. Elsevier. Geomorphology 92. 2007. Pag. 38–59.

Venkatesh Merwade, Aaron Cook, Julie Coonrod. 2008. GIS techniques for creating river terrain models for hydrodynamic modeling and flood inundation mapping. Environmental Modelling & Software. 2008. Pag:1–12.

Villalobos, R., Retana, J., 2001. Un método para Pronosticar Lluvias en Costa Rica: Agrupación de Años con Características Pluviométricas Semejantes para la Creación de Escenarios Climáticos. Gestión de Desarrollo, Instituto Metereológico Nacional. 2001. Pag: 1- 5.

Wei-Chiang Hong. 2008. Rainfall forecasting by technological machine learning models. Elsevier. Applied Mathematics and Computation 200. 2008. Pag: 41–57.

Wieczorek G.F., Wilson R.C. y Harp, E.L., (1985), Map showing slope stability during earthquakes in San Mateo County California: US Geological Survey Miscellaneous Investigations Map I-1257-E, scale 1:62,500.

Wilks. 1998. Multisite generalization of a daily stochastic precipitation model. Journal of Hydrology 210. 1998. Pag: 178–191.

Wilson, L., Huang, T., 1979. The influence of shape on the atmospheric settling velocity of volcanic ash particles. Earth Planet. Sci. Lett. 44, 311-324.

Woods, A., Bursik, M., 1991. Particle fallout, thermal disequilibrium and volcanic plumes. Bull.Volcanol. 53, 559-570.

Young and Sparks 1998, Preliminary Assessment of Volcanic Risk on Monserrat. Monserrat Volcano Observatory Internal Report to UK Government; Vesuvius, Azores – EU-EXPLORIS project, http://exploris.pi.ingv.it/non_comf/ description/index.html)

Young 1998, Volcanic Hazard and Community Preparedness at Volcán Irazú, Costa Rica. British Geotechnical Survey Report WC/98/16R.